

SquirRL: Automating Attack Discovery on Blockchain Incentive Mechanisms with Deep Reinforcement Learning

Charlie Hou*
Carnegie Mellon University, IC3
charlieh@andrew.cmu.edu

Mingxun Zhou*
Peking University
zhoumingxun@pku.edu.cn

Yan Ji
Cornell Tech, IC3
yj348@cornell.edu

Phil Daian
Cornell Tech, IC3
pad242@cornell.edu

Florian Tramèr
Stanford University
tramer@cs.stanford.edu

Giulia Fanti
Carnegie Mellon University, IC3
gfanti@andrew.cmu.edu

Ari Juels
Cornell Tech, IC3
juels@cornell.edu

Abstract—Incentive mechanisms are central to the functionality of permissionless blockchains: they incentivize participants to run and secure the underlying consensus protocol. Designing incentive-compatible incentive mechanisms is notoriously challenging, however. Even systems with strong theoretical security guarantees in traditional settings, where users are either Byzantine or honest, often exclude analysis of *rational* users, who may exploit incentives to deviate from honest behavior. As a result, most public blockchains today use incentive mechanisms whose security properties are poorly understood and largely untested.

In this work, we propose SquirRL, a framework for using deep reinforcement learning to identify attack strategies on blockchain incentive mechanisms. With minimal setup, SquirRL replicates known theoretical results on the Bitcoin protocol. In more complex and realistic settings, as when mining power varies over time, it identifies attack strategies superior to those known in the literature. Finally, SquirRL yields results suggesting that classical selfish mining attacks against Bitcoin lose effectiveness in the presence of multiple attackers. These results shed light on why selfish mining, which is unobserved to date in the wild, may be a poor attack strategy.

Index Terms—Blockchain, Deep reinforcement learning, Incentive mechanisms

I. INTRODUCTION

Blockchains have generated much excitement in the past decade as a method for storing and processing data with *decentralized trust*. Traditional centralized databases (or compute engines) require all users to trust a single party who handles all data processing and storage. If this central party is corrupt, users may be able to detect misbehaving via expensive cryptographic schemes, but cannot actively prevent this from happening. In contrast, blockchains delegate data storage and management to all (or a subset of) participants, who run a *consensus protocol* to agree on the current state of the system. It is theoretically proved that as long as no more than a certain fraction of participants are corrupt, consensus can be reached on blockchain [17], [19], [71]. Unlike the centralized setting, blockchain users don't

rely on a single party to behave honestly, but a proportion of participants to follow the protocol.

The blockchain model of computation requires participants to expend resources (storage, computation, and electricity) to ensure the correctness and liveness of other users' data. These costs can be substantial, depending on both the volume of transactions processed and the details of the underlying consensus protocol. Most public blockchains therefore rely critically on *incentive mechanisms* to motivate users to participate in blockchain consensus protocols. That is, users are typically paid (in native cryptocurrency) to participate in maintaining one another's data.

For example, Bitcoin's consensus protocol requires participants (also known as *miners*) to build a sequential data structure of *blocks*, where each block is forged through a process requiring tremendous computational resources (*mining*). To incentivize participation, Bitcoin miners receive a *block reward* (in Bitcoins) for every block they mine that is accepted by the rest of the network. Miners also receive a smaller *transaction fee* for every transaction they include in a block; this is done to prevent miners from simply mining empty blocks without doing useful work. This incentive mechanism has largely driven the remarkable growth of participation in Bitcoin.

Incentive mechanisms are central to the functionality of most public blockchains; without them, systems cannot survive. As a result, permissionless blockchains (particularly cryptocurrencies) typically have their own incentive mechanism [34], [57], [70]; although many are modeled after Bitcoin's, differences in consensus protocol typically require custom alterations to the incentive mechanism.

A. Attacks on incentive mechanisms

In practice, incentive mechanisms can be susceptible to gaming by participants. For example, *selfish mining* is a well-known attack on Bitcoin's incentive mechanism that allows a strategic miner to reap more than her fair share of block rewards by choosing not to follow the consensus protocol exactly [15].

*Equal contribution

The original selfish mining paper was followed by many papers exploring both attacks on Bitcoin’s incentive mechanism [9], [13], [28], [36], [44], [50] as well as other cryptocurrencies [23], [45], [48].

Today, attacks on blockchain incentive mechanisms are typically discovered through a lengthy process of modeling and theoretical analysis [9], [13], [23], [28], [36], [44], [45], [48], [50]. Moreover, the difficulty of obtaining general theoretical results in this area is well-known [20]. Since many cryptocurrencies lack the resources to do even rudimentary analysis, the vast majority of blockchain incentive mechanisms have not been analyzed at all. This suggests that the substantial amounts of money currently residing in cryptocurrencies may be vulnerable to unknown attacks.

B. Proposed framework: SquirRL

In this work, we propose SquirRL, a framework for discovering attacks on blockchain incentive mechanisms using deep reinforcement learning. SquirRL is intended as a general-purpose methodology for blockchain developers to test incentive mechanisms for vulnerabilities. It does not provide theoretical guarantees: just because it does not find any attacks does not mean that honest behavior is a dominant strategy. We find in practice, however, that instantiations of SquirRL are effective at identifying adversarial strategies, which can be used to prove that an incentive mechanism is *insecure*. Our primary contributions are threefold:

- 1) *Framework*: We present SquirRL as a general framework for exploring blockchain incentive-mechanism vulnerabilities. The framework broadly involves: (1) Creation of a simulation environment, with accompanying state and action spaces reflecting the views and capabilities of participating agents; (2) Selection of an adversarial model, including numbers and types of agents; and (3) Selection of a suitable RL algorithm and associated reward function. In the course of our evaluations, we show how to use this framework flexibly to handle a variety of settings involving varying environments, numbers of agents, rewards, and so forth.
- 2) *Selfish-mining evaluation*: We apply SquirRL to various blockchain protocols. Using SquirRL, we are able to recover known theoretical selfish mining results in the Bitcoin protocol, while also extending state-of-the-art results to domains that were previously intractable (e.g., the multi-agent setting, larger state spaces, other protocols). Our results suggest that in the Bitcoin protocol, as the number of agents increases, selfish mining and its variants become progressively less profitable. This is consistent with the fact that selfish mining has been unobserved in the wild (to the best of our knowledge), although it is unclear whether this observation or other externalities are the reason.

Additionally, our experiments provide results about multi-agent settings that have previously been challenging to analyze theoretically. Prior work deals with these challenges by analyzing simplified strategy spaces [41].

Our experiments empirically consider a richer strategy space, and reveal that the theoretical results of [41] do not extend to the resulting, more realistic model.

- 3) *Demonstration of extensibility*: We show that SquirRL is generally applicable to attacks on incentive mechanisms beyond selfish mining. We apply SquirRL to the block withholding attack proposed in [13]. We show that SquirRL finds two-player strategies that converge to the Nash equilibrium found in that work.

C. Outline of paper

We start by motivating the problem more carefully in §II, and explaining why existing techniques fall short. Next, we discuss some background on deep reinforcement learning in §III, followed by the design of SquirRL is presented in §IV. We evaluate SquirRL on a variety of blockchain protocols and settings, in the single-strategic-agent setting in §V and in the multi-strategic-agent setting in §VI. We conclude with a discussion of shortcomings and future work in §VIII.

II. MOTIVATION

Today, the process for discovering new attacks on blockchain incentive mechanisms is manual and time-consuming. Typically, such attacks require some combination of theoretical analysis, simulation, and intuition [50]. Each becomes more difficult to obtain as the complexity of the underlying protocol grows. In particular, game-theoretic analysis of these systems tends to be challenging for three reasons: (1) the state space is large, (2) the game is repeated, and (3) there can be many agents. Indeed, much of the existing analysis has focused on settings where only one or two agents are allowed to deviate from the honest mining strategy [40].

At the same time, new protocols are emerging frequently, each with its own incentive mechanism [30], [64], [68]. Oftentimes, protocol designers rely on intuition to reason about the security of their incentive mechanisms, in part because we lack general-purpose tools for mechanism analysis. Even in the cases where protocol designers do provide theoretical proofs, they are typically at most stating that honest behavior is a Nash equilibrium (either exact or approximate) [8], [46]. This is a weak guarantee that says nothing about other equilibria or the setting in which multiple parties behave rationally. Our central premise is that a systematic and largely automated approach for testing incentive mechanisms would not only streamline this process, but it could also help catch logical errors in incentive mechanisms *before* protocols are deployed in the wild.

A. Use Case

We envision protocol designers using our framework to study a natural progression of adversarial models and experiments to help address key security/incentive-alignment questions for an incentive mechanism \mathcal{M} . These are shown in Table I.

For a given adversarial resource (e.g., mining power), a *single* strategic agent \mathcal{S} competing against a group of honest agents represents the most powerful possible adversary. (Such an agent

Number of Strategic Agents	Representative Setting	Agent Types	Explored questions
1	Single strategic agent	$\text{Sys} \rightarrow \mathcal{S}$	<ul style="list-style-type: none"> • What impact from worst-case attack? • What is optimal adversarial strategy?
2	Emergent strategic-agent competition	\mathcal{S} vs. Sys	<ul style="list-style-type: none"> • Is \mathcal{S} dominant? • Is \mathcal{S} profitable for competing agent?
		Sys vs. Sys	<ul style="list-style-type: none"> • Is two-agent game stable?
$k \geq 3$	Community of competing strategic agents	$\underbrace{\text{Sys vs. } \dots \text{ vs. Sys}}_{k \text{ agents}}$	<ul style="list-style-type: none"> • Is multi-agent strategic play profitable? • Is \mathcal{H} dominant in multi-agent setting?

TABLE I: Experimental progression in an automated incentive mechanism analysis system Sys. The sequence of experiments with increasing numbers of strategic agents sheds light on key security questions for mechanism \mathcal{M} . Notation $\text{Sys} \rightarrow \mathcal{S}$ is shorthand denoting \mathcal{S} as the output of the automated system.

can simulate any set of strategies among multiple agents.) \mathcal{S} can steal rewards from honest agent \mathcal{H} , whose strategy is fixed *a priori* and thus cannot develop a counter-strategy. Learning \mathcal{S} thus yields insights into the worst-case performance of \mathcal{M} .

Addition of a second strategic agent then addresses the question of whether \mathcal{S} itself is dominant or suboptimal in the presence of a competing agent. This setting captures the dynamics when a single strategic agent is first challenged by others. By training two competing agents in tandem, it is also possible to explore questions such as: How stable are learned strategies over time?

In actual deployment of a mechanism \mathcal{M} , of course a community of $k \geq 3$ competing strategic agents can arise, a case more plausible than sustained attack by a single strategic agent. The SquirRL framework dictates analysis with various values of k to explore the likely *practical* security of \mathcal{M} . For example, a mechanism may have poor worst-case security yet converge to strategy \mathcal{H} for all players given competition among strategic agents. A key question is: How much reward, as a function of k , can strategic agents collectively steal from \mathcal{H} ?

We emphasize that the experiments in Table I are a starting point, not a full prescription. However, they shed light on a number of central, incentive-related questions that are nontrivial to evaluate today.

B. Straw-man solution

A natural first tool for solving this problem is **Markov Decision Processes** (MDPs) and the associated algorithms used to solve them. MDP solvers are commonly used for learning strategies to maximize an agent’s reward in a known but random environment [66]. Indeed, MDP solvers have been used effectively in prior work to computationally learn optimal adversarial strategies in the two-agent setting of the Bitcoin protocol [50].

MDPs are defined as a tuple (S, A, P, R) , where S denotes a finite set of states, A denotes a finite set of actions the agent can take, P denotes the probability transition matrix, where $P_a(s, s') = \mathbb{P}(s_{t+1} = s' | s_t = s, a_t = a)$ denotes the probability of the agent transitioning to state s' from state s by taking action a . R is the reward matrix, where $R_a(s, s')$ denotes the expected reward associated with transitioning from state s to s' by taking action a . We highlight two aspects of this definition.

First, it relies critically on a Markov assumption, which states that the probability distribution over states depends only on the previous state and the action taken at each time step. Second, this formulation requires us to know the associated probability transition matrices. Conditioned on these assumptions, the objective in an MDP is to recover a strategy π that optimizes the expected discounted long-term reward $\mathbb{E}[\sum_{t=0}^{\infty} \eta^t R_{a_t}(s_t, s_{t+1})]$, where $\eta \in (0, 1)$ is a discount factor that accounts for how much the agent values short-term rewards over long-term ones, and the expectation is taken over the randomness in the system evolution and the potentially randomized strategy π .

There exist well-known techniques for solving MDPs numerically, such as value iteration and policy iteration. In [50], these techniques are used to find an optimal selfish mining strategy for a rational Bitcoin agent with fraction α of the system hash power who aims to maximize his relative rewards compared to another honest agent with $(1 - \alpha)$ -fraction hash power who follows the Bitcoin protocol. Here, relative rewards refers to the fraction of main-chain blocks mined by the adversary. However, MDP solvers exhibit two primary constraints that prevent them from being a useful general-purpose tool for our problem.

1. *MDP solvers require an accurate model of the environment.* In other words, to formulate the problem as an MDP, we need to know the probability transition matrix P . This is feasible in the two-agent blockchain setting where one agent is honest, because we know how the honest agent will behave, so the only randomness lies in which agent will produce the next block. However, in practical settings, we may have multiple rational agents who are dynamically changing their strategies over time and/or a changing environment. Although there exist extensions of MDPs designed to deal with hidden state (partially-observed MDPs, or POMDPs [26]), these extensions do not deal with the scenario where the environment is changing over time.

2. *MDP solvers are computationally tractable only for constrained problems with a (relatively) small state space.* For example, in Bitcoin, [50] formulates an MDP where the state space is captured by entirely by three variables: the length of the adversarial private fork, the length of the honest fork (relative to split between the adversarial fork and the main chain), and a relevance variable that can take one of three values. MDPs require storage that scales as $O(|n|^2)$ for a state

space of size n , which can be prohibitive for protocols with larger state spaces, such as DAG-based protocols [34], [57], [70].

III. DEEP REINFORCEMENT LEARNING

Reinforcement learning (RL) is a class of machine learning algorithms that learn strategies enabling an agent to maximize her cumulative rewards in an environment. Although MDPs are central to the study of RL, the field encompasses more general settings as well. In particular, *deep reinforcement learning* is a class of RL that uses neural networks to learn policies, often without needing to explicitly specify the underlying system dynamics [16]. In this work, we explore the potential of deep reinforcement learning to automate the discovery of attacks on blockchain incentive mechanisms, particularly in settings where MDP solvers are impractical or impossible to use, e.g., in the model-free setting.

Deep RL has been particularly successful in problems that exhibit two properties: (1) the rules are well-defined, and (2) the state space is intractably large. Widely-publicized examples like chess and Go exhibit both of these properties [53], [54], as do blockchain incentive mechanisms. In fact, the blockchain incentive mechanism problem has an additional advantage in that blockchain rewards are processed continuously. That is, in chess or Go, rewards are calculated in an all-or-nothing manner at the end of the game. In blockchains, players typically reap rewards for every block they add to the ledger; this allows players to estimate their rewards before the game is complete, which makes it easier to train automated systems to learn effective strategies by providing faster feedback. As such, deep RL is a natural tool for this problem.

There are a few common ways of categorizing RL problems [16]. In *model-based learning*, a probabilistic model of system dynamics is either given or estimated, and policies are learned from this model; classical MDPs are an example. In this work, we are more interested in *model-free learning*, where the agent must learn directly by interacting with the environment, without access to a model. This scenario is more applicable to blockchains because the environment dynamics may be changing over time. Within model-free learning, there are two primary techniques for learning strategies: value-based methods and policy gradient methods [16]. Value-based methods typically aim to build a *value function* that associates some value with each state; a common example is Q-learning [65]. Policy gradient methods instead try to optimize rewards by performing gradient ascent on a parametric policy, which in our case will be represented by a neural network [16]. Common examples include the REINFORCE algorithm [67]. We make use of both classes of algorithms in this work.

A. Technical challenges

Using deep RL effectively involves a number of design decisions that depend on the structure of the underlying problem.

(1) *State representation*. Most blockchains are structured as a directed acyclic graph (DAG), so a naive state representation

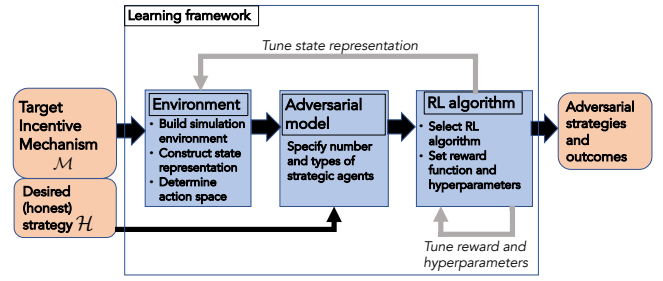


Fig. 1: Schematic of SquirRL learning framework.

might be to use this entire structure as the state representation (including the agent’s local information). This approach has a few problems. First, its dimensionality grows over time, causing the overall dimensionality to become prohibitively high. Second, it includes irrelevant information. In any blockchain that provides common security properties like the common-prefix property [17], blocks embedded deep in the blockchain are permanent with high probability. Hence, a rational player cannot displace them, so including them in the state representation is wasting computation and representational power. Designing a system to attack blockchain incentive mechanisms therefore requires a state representation that is general enough to apply to many different types of blockchains, while being constrained enough to limit the problem dimension.

(2) *Learning algorithm*. There are many deep RL algorithms, and different ones perform well in different settings. The most basic algorithm is deep Q-networks (DQNs), which is based on the classical idea of Q-learning [65]. However, more sophisticated algorithms have surpassed DQNs in many problem areas [32], [51], [72], at the expense of higher computational cost. Choosing which learning algorithm to use therefore requires some domain expertise.

(3) *Reward function*. Designing a good reward function can significantly impact the success of the overall system; often this requires a combination of domain knowledge and some tuning.

(4) *Hyperparameters*. As with many deep neural networks, deep RL involves a number of hyperparameters, such as the learning rate and the architecture of involved neural networks, that can affect both convergence rates and the strategies we can learn.

Next, we discuss how SquirRL navigates this design space in Section IV.

IV. SQUIRRL: SYSTEM DESCRIPTION

Figure 1 shows use of the RL-based *learning framework* that is the cornerstone of SquirRL. This framework involves a three-stage pipeline for discovering and analyzing adversarial strategies targeting an incentive mechanism \mathcal{M} .

First, the protocol designer builds an *environment* that simulates execution of the protocol realizing \mathcal{M} . We anticipate that the bulk of the effort involved in the SquirRL framework will typically go into this part of the system, as the environment

fully encapsulates a model of \mathcal{M} . The protocol designer instantiates in the environment a *state representation* over which learning will occur, as well as a space of *actions* that agents may take. (The state representation may be iteratively tuned to improve performance of the RL algorithm at later stage.) Next, the protocol designer chooses an *adversarial model* to explore. We have outlined a principled set of choices in our discussion of Table I in Section II. Finally, the protocol designer selects an *RL algorithm* that is appropriate for the environment and adversarial model. She must associate with the RL algorithm a reward function and hyperparameters, both of which may be iteratively tuned as exploration proceeds.

In this section, we describe respectively the environments, adversarial models, and RL algorithms we employ in our use of SquirRL for the experiments in this paper. We then give a brief overview of the system architecture that realizes these choices.

A. Environment Design

We focus in this paper mainly on selfish-mining-type attacks in proof-of-work systems, since these have dominated the literature on blockchain incentive mechanism vulnerabilities [15], [23], [41], [44], [50]. We therefore describe how we construct our environment for such attacks. Naturally, the environment construction differs slightly based on the precise incentive mechanism (and underlying consensus algorithm), but there is a strong commonality among our environment designs. Our techniques can also be generalized to non-proof-of-work systems, and other types of attacks (some of which have been observed in the wild [13]). As an example, we demonstrate the applicability of RL to another attack class, block withholding, in Section VI-E.

a) *Blockchain generation*: For simplicity, we start by explaining the simplest setting used to run the single-agent experiments. This model is generalized in later sections of the paper. As in prior work [15], [50], much of our work assumes a randomized model for block generation where the network communicates blocks instantaneously to all other nodes. Hence, we view block generation as a discrete-time process, where a new block is generated at each time slot $i \geq 0$. A party that controls fraction α of the network's hash power mines the i th block with probability α , independently across all time slots.

Several (but not all) of the models we study are *greatest-work* protocols, which we model for simplicity as longest-chain protocols. This means that every time an honest node produces a block, it chooses to append the block to the longest valid chain of blocks in the public blockchain. In the event of multiple longest chains of equal length (e.g., if an adversary publishes a new block at the same time as the honest nodes), we assume the honest nodes all follow the adversarial longest chain with probability γ , and all follow the honest longest chain with probability $1 - \gamma$. We call this parameter the *follower fraction*.

b) *Rewards*: In most chain-based blockchains (e.g., Bitcoin), the miner of a block that appears in the final ledger receives a token *block reward* for its efforts. The environment assigns block rewards to agents, which can differ in general

from instantaneous rewards in the learning framework. Like prior work in this space [15], [44], [50], we consider one or more attackers that aim to maximize their block rewards given a constrained amount of computational resources; we ignore the role of transaction fees for simplicity. We define $B_a(t, p)$ and $B_h(t, p)$ as the rewards of the attacker and the honest miners, respectively, at time t under an attacking strategy p . When there are multiple attackers, we differentiate them with superscripts. We compute a miner's reward by aggregating the amount of block reward it accumulates, avoiding analysis of uncontrolled externalities such as coin price or electricity cost.

In practice, miners appear to optimize their **absolute reward rate**, defined as $\frac{B_a(t, p)}{t}$. However, prior work [15], [50] has mostly focused on **relative rewards**, defined as the attacker's block rewards as a fraction of the whole network's rewards: $\lim_{t \rightarrow \infty} \frac{B_a(t, p)}{B_a(t, p) + B_h(t, p)}$. This discrepancy has led to discussions about the practicality of selfish mining [14]. In the following, we clarify the relationship between absolute reward rate and relative reward, and show that over even moderate time periods in the Bitcoin protocol, the two objectives are interchangeable.

The **difficulty** of a block is the average computation required to mine it. If the computational power of the whole network increases or decreases, the block difficulty increases or decreases accordingly to maintain a target block generation time under dynamic network conditions. For instance, in Bitcoin, the target main chain block generation rate, a.k.a. growth rate, is $T_0 = 10$ minutes/block, and the difficulty is adjusted every $M = 2016$ blocks; we call this duration an *epoch*. The difficulty d' of one next epoch is adjusted according to the current difficulty d and the average main chain growth rate T of current epoch, such that $d' = d \frac{T_0}{T}$.

We next show that over n epochs with difficulty adjustment, the absolute reward rate (scaled by a constant) and relative reward are close to one another for a single strategic agent competing against an honest agent. In what follows, we let S_a and S_h denote the number of adversarial and honest stale blocks in a single epoch, respectively; a stale block is a block that does *not* end up on the main chain, and hence does not collect any block reward. Note that the following result relies on the deterministic analysis of [21], which abstracts away the stochastics of the problem.

Proposition IV.1. *Let R_n denote the expected absolute reward rate over n epochs, \tilde{R}_n the expected relative reward rate, and T_0 the target (expected) inter-block time. Consider an attacker with $\alpha < 0.5$ fraction of the total hash power in the network. We assume that 1) the attacker always uses all its mining power, 2) the attacker uses the same strategy across all epochs, and 3) the total hash power of the network remains unchanged across epochs. Then under a deterministic analysis model,*

$$R_n = \frac{1}{T_0} \frac{B_a}{(B_a + B_h) + \frac{1}{n}(S_a + S_h)}, \quad (1)$$

which in turn implies that $|T_0 R_n - \tilde{R}_n| \leq \frac{1}{n}$.

The proof can be found in Appendix A. Proposition IV.1 has two main implications. The first is that over the course

of a single epoch, honest mining is an optimal strategy for maximizing the absolute reward rate; selfish mining is actually less profitable. This follows because to maximize the absolute reward in (1), the denominator should be minimized. This can be achieved by producing no stale blocks, which occurs under honest mining.

The second implication is as follows: since maximizing absolute reward rate is equivalent to maximizing absolute reward rate scaled by a positive constant (T_0), Proposition IV.1 suggests that for moderate n , the objective functions for optimizing relative rewards and absolute reward rate are provably close. In particular, we have that

$$\lim_{n \rightarrow \infty} R_n = \frac{\tilde{R}_n}{T_0},$$

i.e., in the infinite-time horizon, optimizing absolute reward rate is equivalent to optimizing relative rewards. SquirRL can be used to optimize both absolute rewards and relative rewards; however, to compare with prior literature and because of this asymptotic equivalence, we start by considering relative rewards.

Rewards in multi-agent setting. In the multi-agent setting, rewards should not be immediately handed out following an override or adopt action. This is because unlike the single-agent setting, there is still a possibility of the strategic party's chain being overridden by another strategic party. Hence, our system only gives a block reward if all agents acknowledge the block, i.e., by adopting it.

Additional parameters. Depending on the protocol and experimental setting, more parameters may be required to specify environment execution. For instance, in our experiments on the GHOST protocol, we have an additional *stale block rate* parameter.

c) Action space: We allow miners to take one of four basic actions, as in [15], [50]. The first is **adopt**. The adopt action means that an attacker abandons its private fork to mine on the longest public fork. This action is always allowed. The second action is **override**. An attacker that overrides is publishing just enough blocks from its private chain to exceed the length of the longest public chain. This action is feasible only if the agent's private chain is strictly longer than the public main chain. The third action is **wait**. An attacker that waits continues to mine, but does not otherwise alter its state. This action is always feasible. The fourth and final action is **match**. An attacker that matches publishes just enough blocks to equal the length of the longest public chain and cause a forking race condition. As needed, we will modify these actions to accommodate different protocols.

d) State space: The state space for each of our environments is slightly different, but they all derive from that defined in [50], as all the protocols we investigate are similar to the Bitcoin protocol. Let $\{a, h, fork\}$ be the tuple defining the state that an attacker sees at a given time step t . Here, a denotes the number of blocks the attacker has in its fork, counting from the last common block between both agents, h is the length of the longest public fork, and $fork$ is the forking characteristic.

A state of the form $\{a, h, relevant\}$ means that the previous state (at time $t-1$) was $\{a, h-1, \cdot\}$, where \cdot means the entry can take any value. This means that an honest block was mined in time step t , so as long as $a \geq h$, a *match* action is feasible. To avoid computing an infinite-dimensional MDP, we adopt a similar truncation technique to that of [50], which limits any fork's length to B_{max} , i.e. $a, h \leq B_{max}$. Unless specified otherwise, we set B_{max} to 20 in our experiments.

Similarly, a state of the form $\{a, h, irrelevant\}$ means the previous state was $\{a-1, h, \cdot\}$; since a match requires the agent to publish its block in the same time step as another agent, a match is not possible when $fork = irrelevant$ because the latest honest block was already been broadcast in the previous time step $t-1$. The state $fork = active$ means that the attacker is in a forking race condition; that is, it matched with the honest party in the previous time step, and is currently waiting to learn if it will be able to overtake the honest branch. As needed, we add additional information to this state space based on the setting. For instance, Ethereum extends this state space to account for uncle blocks.

e) Action sequencing: An important adjunct to design of the action space is a policy for the *sequencing* of agents' actions. In our environment design, we enforce two properties: (1) *Synchronous action selection.* We assume all actions of strategic agents are recorded synchronously, after seeing the actions of the honest party (if it exists). This is needed to prevent the adversary from observing the actions of other strategic players and reacting accordingly; in this case, the last strategic agent to choose its action would have an unfair advantage. However, we do allow for a rushing adversary who sees the honest party's actions before deciding how to act.

(2) *Delayed execution of adopt.* Once actions are recorded, we must apply them in some order. We have chosen always to apply the adopt action last. To see why, consider the following scenario: suppose an honest agent is mining on the public chain in the presence of two strategic players, 0 and 1. Now suppose agent 0 overrides and agent 1 adopts. We know that actions are collected synchronously, but if they were also *processed* synchronously, agent 0's chain would become the main chain, while agent 1 would have adopted the previous main chain, which is now stale. This behavior is unrealistic because a truly strategic player 1 would choose to mine on player 0's override block if it were to abandon its private chain. This problem arises frequently with adopt actions, thus motivating the need to treat this action differently.

B. Adversarial model

In our experiments on selfish mining in Sections V and VI, we explore the numbers and types of adversaries given in Table I. We consider only two agents for the case of block withholding in Section VI, as the literature on realistic environment modeling is less mature.

The type of each agent i in our various experiments is specified in part by an associated (fractional) hash power α_i . In our self-mining experiments, agent types include two additional parameters: (1) an agent-specific "follower fraction" γ_i that

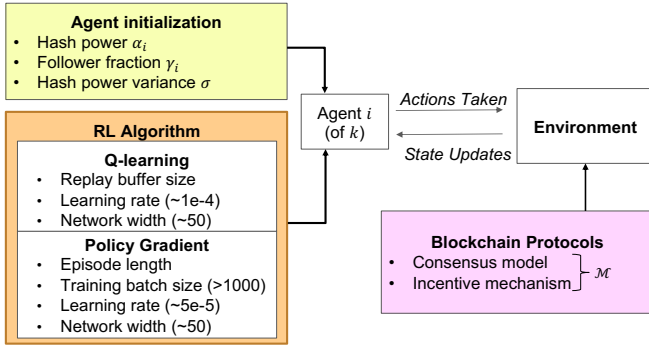


Fig. 2: Detailed system design for SquirRL. Each agent uses one RL algorithm, which can differ across agents. In our experiments, all agents used either DDQN or PPO.

specifies the probability that honest nodes follow a particular agent’s chain in the case of multi-way ties; this parameter models an agent’s network penetration and is described further in Section VI, and (2) an upper limit B_{max} on the number of private chain blocks allowed before agents are forced to mine honestly. This upper limit models the fact that blockchain communities may ignore large chain reorganizations [69].

C. RL algorithm

We employ different deep reinforcement learning algorithms, depending on the adversarial model. In the single agent setting, we use Deep Dueling Q-Networks (DDQN) [62] and in the multiple agent setting, we use Proximal Policy Optimization (PPO) [51]. DDQN is a Q-learning method that estimates the expected value of an action given the state. These types of algorithms require the expected value of an action given a state to be constant when the policy is fixed (Markov assumption) in order to converge. In our experiments, we have found that DDQN converges faster than PPO in the single agent setting for Bitcoin: with a block limit of 5, $\alpha = 0.4$, $\gamma = 0$, DDQN converges in roughly 10^5 steps in the environment, while PPO takes an order of magnitude more steps to converge.

However, DDQN can fail when there are multiple adaptive agents because the Markov assumption no longer holds. Policy gradient methods are more resilient to deviations from the Markov assumption, so we use PPO in the multiple agent setting for selfish mining.

D. Architecture

We used OpenAI Gym [7] to construct our environments and execute RL algorithms on them. In Figure 2, we illustrate the particulars of our system architecture given our design choices within the SquirRL framework. We highlight in colored boxes the parts of the architecture that are configurable through explicit interfaces and require some input from the system operator.

OpenAI Gym provides a generic interface for implementing environments. In our case, this environment represents a combined blockchain consensus mechanism and block reward structure, which together specify the target incentive mechanism

\mathcal{M} . The environments we have implemented provide a template for users to easily instantiate their own blockchain protocols (namely, blockchain structures ranging from pure chains to generic DAGs).

As we frequently vary the parameters (hash power, etc.) specifying agent types, we include in our architecture an explicit agent initialization interface. This interface also allows agents’ hash powers to be varied stochastically over time—a feature that usefully reflects the dynamic conditions of real-world mining.

Finally, our architecture supports multiple RL algorithms, such as DQN, PPO, A2C, and policy gradient. Different agents can be initialized to use different RL algorithms. However, we found empirically that DDQN and PPO worked well for a wide range of experiments; we discuss these tradeoffs more in Section IV-C.

V. EVALUATION: SINGLE STRATEGIC AGENT

We evaluate SquirRL by following the pipeline proposed in Section II, starting with a single strategic agent. We first consider applications of SquirRL to selfish mining attacks for a number of major protocols including Bitcoin and Ethereum, while also providing visualizations and analyses that may help protocol designers understand the weaknesses in incentive mechanisms. Experiments for additional parameter settings are included in Appendix A.

The single-agent setting is characterized by a single adversarial party, assuming all remaining agents are honest [15], [44], [50]. This was the setup initially used to show that Bitcoin is susceptible to selfish mining attacks [15]. In this section, we use the same setup to study various important blockchain incentive mechanisms, including Bitcoin, Ethereum, and GHOST. Our experiments in this section compare several baseline mining strategies:

- (1) **Honest mining**: a miner who follows protocol.
- (2) **Optimal selfish mining (OSM)**: the strategy learned in [50] for the Bitcoin protocol. More generally, in cases where we can write out an MDP for the system, we will alternatively use the acronym **MDP** to denote the optimal solution.
- (3) **SM1**: the selfish mining strategy originally proposed in [15]; although this baseline should be strictly dominated by OSM in the Bitcoin setting, it has been used in other settings as well [45]; we include it for completeness.
- (4) **RL**: the proposed system, SquirRL.

In each of our experiments, we train each baseline to completion. Then, for a given parameter setting (e.g., initial adversarial party’s fraction of hash power α), we run 100 trials of each blockchain protocol, where each trial consists of 10000 status transitions and at least 5000 blocks in the main chain. We compute the relevant parties’ rewards for each trial, and average over all trials.

A. Bitcoin

The Bitcoin protocol is a useful case study in part because its incentive mechanism is well-studied [13], [15], [44], [50]. In particular, prior work has recovered an *optimal* selfish mining strategy in the two-party case [50]. A useful sanity check

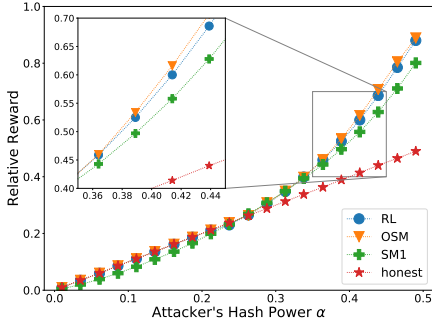


Fig. 3: Bitcoin relative reward as a function of adversarial hash power. SquirRL recovers the findings of [50].

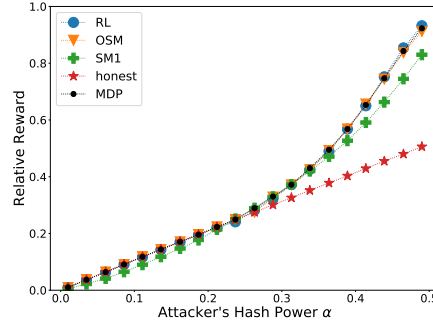


Fig. 4: GHOST relative reward as a function of adversarial hash power. Stale block rate is fixed to 6%.

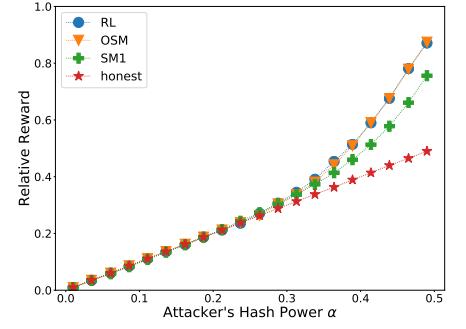


Fig. 5: Ethereum relative reward as a function of adversarial hash power. RL beats state-of-the-art schemes.

is therefore to see if SquirRL recovers these known optimal results. In [50], the authors recover the optimal strategy for selfish mining in Bitcoin by posing the problem as an MDP and solving it numerically with an MDP solver. We aim to recover and replicate two key findings of their work:

- (1) Selfish mining is only profitable only for adversaries who hold at least 25% of the stake in the system; this assumes that if the adversary publishes a block at the same time and height as the honest chain, the honest nodes will build on the adversary's block with probability $\gamma = 0.5$. An adversary who holds less than this fraction should revert to honest mining.
- (2) For adversaries with more than 25% of the stake, the authors show performance curves that quantify by how much the adversary can amplify its relative rewards compared to honest mining. Our goal is to match these curves.

Figure 3 demonstrates the outcome of this experiment. We observe two key findings. First, for $\alpha < 0.25$, SquirRL does not adopt a 'selfish mining' strategy, but recovers the honest mining strategy. This sanity check is consistent with the theoretical findings of [50]. Second, for $\alpha > 0.25$, we find that SquirRL achieves a relative reward within 1% of the true optimal mechanism. This result required minimal tuning of hyperparameters.

B. GHOST

We also evaluate these techniques on the GHOST protocol [57]. Although GHOST is not directly used in existing cryptocurrencies, it is being considered for adoption in Ethereum [1], [2]. It is also an interesting setting since its state space is much larger than Bitcoin's.

The protocol is as follows: each miner builds blocks not on the *longest* chain, but on the *heaviest subtree*. As the miner starts traversing the blocktree from the genesis block, each time it encounters a branch, it chooses the subtree with more total blocks. Honest miners mine on the longest chain of the heaviest subtree; for these experiments, we assume that block rewards are accrued only for blocks mined on this longest chain.

Modeling GHOST has two main differences compared to modeling Bitcoin. The first is that one can no longer simply

keep track of branch lengths in the state space. The new state space is defined by $(a, h, fork, h_w)$, where h denotes the longest branch of the public subtree and h_w denotes the weight of the public subtree. In this case, only when the attacker's private fork's weight is larger than the public branch's subtree, i.e. $a > h_w$, is the 'override' action feasible.

The second difference is that our environment must be designed to model increased forking in the blockchain. To this end, we adopt the concept of a 'stale block rate' from [18]. Due to network latency, honest miners generate **stale blocks**, which are not mined on the tip of the longest public chain. We model this with a parameter $\xi \in [0, 1]$, which captures the probability of a mined honest block being mined not on the tip of the heaviest chain. Notice that a stale block only affects the weight of the public heaviest subtree, not the length of its longest chain. This is captured by incrementing the extra parameter h_w in the state vector, which denotes the weight of the public subtree. With probability $1 - \xi$, an honest block is mined on the tip of the heaviest subtree, so both h and h_w are incremented.

a) *Performance.*: Figure 4 shows the relative rewards of our different baselines as a function of adversarial hash power α . As with Bitcoin, we observe that RL substantially outperforms both honest mining and the SM1 strategy. We also observe that RL has comparable relative rewards to the MDP curve, which is optimal. Perhaps surprisingly, OSM also has a similar reward to MDP, suggesting that the GHOST protocol may not be different enough from Bitcoin to produce different results.

These GHOST experiments are useful for quantifying the differences in computational requirements between MDP solvers and deep RL. MDP solvers require a complete probability transition matrix and reward matrix, which have space complexity $O(n^2)$ in general, where n is the size of the state space. Recall that we truncate the state space to avoid an infinite-dimensional MDP. In the GHOST setting, with the extra dimension in our state, the state space grows cubically in the truncation threshold B_{max} , where B_{max} denotes the maximum value of each entry in the state vector. When we set $B_{max} = 30$, the the state space has 21,763 possible values, and the MDP solver requires around

7GB memory. Moreover, when $B_{max} = 100$, the state space size is 707,203 and the MDP solver needs more than 8TB memory. On the contrary, the RL does not rely explicitly on the state transition tables. The major component of the RL neural network contains two fully connected layers with 100 hidden nodes and the whole network requires only 0.4MB memory. SquirRL robustly learns a good strategy even when the state space is big, achieving a relative reward within 1% of the OSM strategy (even for $B_{max} = 100$).

C. Ethereum

Our third experiment uses the Ethereum incentive mechanism. Ethereum’s incentive mechanism is similar to Bitcoin’s, except for its use of *uncle rewards*. If a block is not a main chain block but a child block of a main chain block, it can be referenced as an *uncle block* (Figure 6). Each block can point to at most two uncle blocks; it obtains $\frac{1}{32}$ of the full block reward for each uncle-block pointer. In addition, the miner of the uncle obtains a $\frac{8-k}{8}$ ($1 \leq k \leq 6$)-fraction of the full block reward, where k is the height difference between the uncle block and the nephew block that points to it.

State space. Recall the state space for the Bitcoin setting is defined by the tuple $\{a, h, fork\}$. For Ethereum, we introduce an extra 6-dimensional vector $U = \{u_1 \dots u_6\}$ to the state space to represent uncle block information. $u_i \in \{0, 1, 2\}$ records the information of the uncle blocks hanging on the main chain block of height $H - i$, where H is the current height of the last common block of the main chain (Figure 6). $u_i = 0$ means there are no uncle blocks at that height. $u_i = 1$ and $u_i = 2$ mean that an uncle block hanging from the main chain at height $H - i$ was mined by the attacker or honest miner, respectively. For instance, in Figure 6, the attacker holds a secret fork with 2 blocks, while the public fork has only 1 block. The height of the main chain is $H = 4$, and there are two uncle blocks mined by the attacker hanging from blocks of height 1 and 3. The uncle block mined by the honest miner is hanging at height 2. So the uncle vector is $U = \{1, 2, 1, 0, 0, 0\}$. Unfortunately, this state space is too big for most MDP solvers. For example, if we limit the maximum number of hidden blocks to 20, the state space size will be around 291,600. Therefore, RL can be a powerful tool in this setting.

Reward. When an Ethereum block is generated, the miner includes references to any uncle blocks. Including these uncle references into the state space would cause a multiplicative (and unnecessary) increase in the state space size. To deal with this, during the learning process, we postpone accounting for the uncle references until a block is confirmed as an uncle or main chain block by both the attacker and the honest miner; our environment, however, implements uncle references instantly, as in the Ethereum protocol. Figure 7 shows an example. The attacker publishes its secret fork of 2 blocks to override the public fork, and it can gain additional rewards by referring to the hanging uncle blocks. We hard-coded an uncle selection strategy for both the attacker and honest miner: 1) both agents select the oldest available uncle block(s) first; 2) the honest miner refers to all feasible uncle blocks, starting with the oldest

Name	Strategy			
	Honest	SM1	OSM	RL
Bitcoin	0.39	0.53	0.55	0.58
Litecoin	0.40	0.54	0.58	0.59
Dogecoin	0.40	0.53	0.56	0.57
Vertcoin	0.34	0.44	0.46	0.47

TABLE II: Relative rewards under stochastic α as measured in real cryptocurrencies from September 8-October 13, 2018. Results shown for initial $\alpha = 0.4$.

one; 3) the attacker only refers to uncle blocks mined by itself, to increase its own relative reward. For example, in Figure 7, the attacker will refer to its own uncle blocks hanging at heights 1 and 3 in its first block, and omit u_2 because it is a honest miner’s block. As such, the attacker gets the extra inclusion reward and two uncle block rewards that add up to $\frac{1}{32} + \frac{7}{8} + \frac{5}{8} = \frac{49}{32}$ block reward.

State updates with uncles. The additional uncle state does not affect state transitions for the 3-tuple $(a, h, fork)$. Therefore, we only need to define updates to the uncle state vector. As noted, this vector only changes when a new block is confirmed by both the attacker and the honest miner on the main chain. When this happens, the uncle state vector changes in three ways. 1) Any referred uncle blocks are removed from the vector by setting their corresponding entries to 0; this prevents future blocks from referring to these already-referred uncle blocks. These uncle blocks can safely be removed because both parties have already agreed on a main chain that includes the referred uncle blocks; hence there is no possibility of the main chain later forking in such a way that previously-referenced uncle blocks are no longer referenced. 2) As the main chain’s height is growing, the uncle indices are shifted, and any uncle blocks deeper than depth 6 are discarded, since they cannot be referred by any future blocks. 3) Any fork shorter than the main chain is abandoned, and its first block becomes a new potential uncle block.

a) *Performance:* Figure 5 compares the relative rewards obtained by SquirRL to other literature on selfish mining attacks in Ethereum [23], [45], [48]. We find that SquirRL outperforms all prior literature on selfish mining in Ethereum. This is in part because prior literature has considered only constrained strategies that are effectively equivalent to SM1. For example, [48] only performs a Monte Carlo simulation of SM1, while [23], [45] design different Markov process to analyze SM1 in Ethereum. In fact, it turns out that Bitcoin OSM also outperforms prior works, as shown in Figure 5. Here we were unable to recover the true optimal solution (MDP) as the full Ethereum state space is too large for an MDP solver. This example illustrates how SquirRL can be used to explore the strategy space in scenarios where we do not have *a priori* intuition about what strategies perform well and when MDP solvers are unable to recover meaningful results.

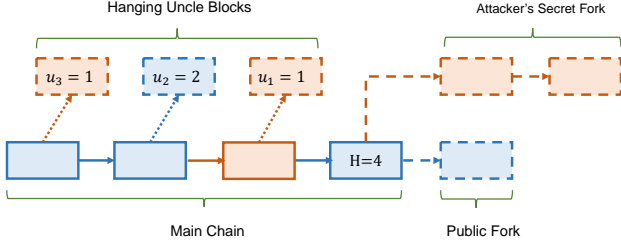


Fig. 6: Ethereum state $(2,1,\text{irrelevant})$ and $U = \{1,2,1,0,0,0\}$. Orange blocks are mined by the attacker and blue blocks by the honest miner.

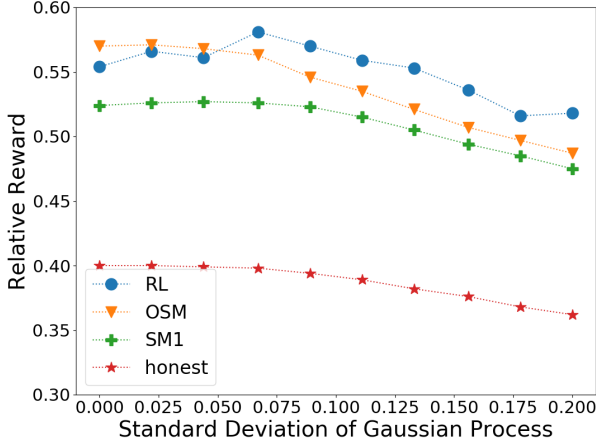


Fig. 8: Bitcoin relative reward under stochastic α (Gaussian random process).

D. Variable Hash Power

In the previous three experiments (Bitcoin, GHOST, Ethereum), it is possible to write an MDP approximating the system dynamics (even if the state space is large). In more realistic blockchain settings, the underlying MDP may be changing over time or unknown. In this section we explore such a scenario, where the adversary's hash power α changes stochastically over time. This can happen, for instance, if the adversary maintains a fixed amount of hash power (in megahashes/day) while the total hash power in the cryptocurrency fluctuates, or if miners dynamically re-allocate hash power over time to different blockchains [31], [43]. In either scenario, formulating an MDP is challenging for two reasons: (1) We may not know the distribution of random process $\alpha(t)$; (2) Even if we can estimate it (e.g. from historical data), incorporating this continuous random process into an MDP would bloat the state space, particularly if fluctuations are not well-captured by the Markov property.

SquirRL handles this uncertainty by using the current value of α during training without any knowledge of the underlying random process. Surprisingly, we find that SquirRL learns to predict fluctuations in $\alpha(t)$, and is therefore less likely to

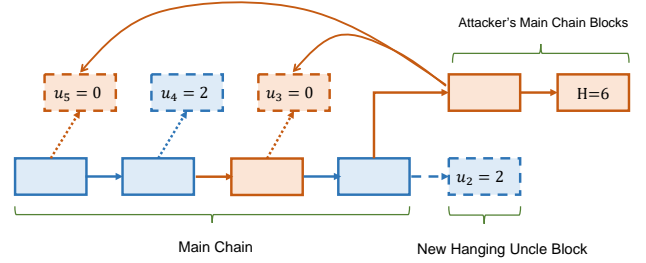


Fig. 7: Ethereum state $(0,0,\text{irrelevant})$ and $U = \{0,2,0,2,0,0\}$. The attacker overrode the public fork with its secret fork and referred to two uncle blocks.

overreact to outlying values.

We evaluate performance for stochastic α by first allowing $\alpha(t)$ to vary according to a Gaussian white noise random process with $\mathbb{E}[\alpha(t)] = 0.4$. Figure 8 illustrates the relative reward as a function of the standard deviation of this process. We truncate fluctuations to $\alpha \leq 0.5$ to avoid 51% attacks. We first observe that when $\alpha(t)$ has low variance, our results are consistent with those from Section V-A: SquirRL achieves relative rewards that are close but not identical to OSM. However, as the variance increases, we observe that SquirRL actually starts to outperform OSM. Intuitively, the learned strategies are less likely to react to fluctuations in $\alpha(t)$, thereby preventing the agent from taking extreme actions for anomalous events. We would consequently expect SquirRL to perform particularly well on blockchains with low (and hence more volatile) total hash power.

To explore the effect of stochastic α in the wild, we ran SquirRL on data from real cryptocurrencies. We first trained SquirRL in an environment where $\alpha(t)$ followed a Gaussian white noise random process with standard deviation 0.1. We chose this standard deviation prior to seeing the data from real cryptocurrencies. Next, we scraped the estimated total hash power in the system once an hour for at least 10 weeks for four different PoW-based blockchains: Bitcoin, Litecoin, Dogecoin, and Vertcoin. All of these blockchains use Bitcoin's consensus protocol and block reward mechanism. We then assumed an attacker with constant raw hash power (in MH/day); this raw hash power is chosen by initializing the attacker at a relative hash power of $\alpha = 0.4$ in each measured blockchain. Once the absolute hash power is fixed, the attacker's relative hash power α fluctuates over time solely due to changes in the total hash power of each blockchain. Table II shows the relative rewards resulting from using various strategies. SquirRL outperforms alternative strategies in terms of relative reward, illustrating RL's benefits in environments that change in ways difficult to capture with an MDP.

VI. MULTI-AGENT EVALUATION

The previous section shows that in the single-agent setting, a properly-instantiated RL agent can learn near-optimal strategies in settings with a well-defined MDP, as well as surpassing state-of-the-art strategies in settings where the environment

is changing stochastically over time. We expect that protocol designers can use similar experiments to test new protocols.

The single-agent setting, however, can be too conservative in practice, as noted in Section II. Blockchains are designed for use by many independent parties, and multiple strategic agents are likely to arise and compete. Results from the single-agent setting may therefore overestimate the gains achievable by strategic agents in practice. At the same time, the multi-agent setting is difficult to analyze theoretically, and explicitly defining an MDP is infeasible due to time-varying, unknown strategies. RL techniques are, in contrast, a natural fit.

In this section, we study the effects of having multiple parties compete in the Bitcoin protocol, both in selfish mining and block withholding attacks. As we focus mainly on selfish mining in this work, we start by explaining the model and setup for those experiments.

Model. Now that we are dealing with more strategic parties, we must generalize some of the notation from Section IV-A. In particular, recall that for a single strategic agent, we used γ to denote the probability of the honest party choosing an adversarial block over an honest one in the event of a match. For the multi-agent setting, we instead define the *follower fraction* γ_i , which we briefly described above. Specifically, for $i \in \{1, \dots, k\}$, γ_i is the probability of the honest agent building on the i th agent’s block in case of a k -way tie. This models each party’s connectedness in the network. In case of a tie among fewer parties, the γ_i values are normalized appropriately.

Training Methodology. As explained in Section IV-A, policy gradient methods like PPO are better-suited to experiments in the multi-agent setting, though there are a few subtleties. Policy gradient methods use “rollouts” [59]—or the full action-state sequence in a training episode—to estimate (1) the gradient of the policy’s performance with respect to the policy parameters, and (2) the value function. As a result, episode lengths should be limited during training; if we keep episodes at 10,000 block creation events (i.e., the length of a trial in the single agent case), the agent often struggles to attribute an observed outcome to a particular action. Based on empirical tuning of this hyperparameter, we settled on an episode length of 100. Aside from this hyperparameter, we used the default assignments for training parameters from [35] for PPO, adapting the number of workers to the number of CPUs on our machines.

Experimental Setting. Each training iteration consists of 28,000 block creation events in the environment; this number was chosen to fully utilize the hardware available to us, which consists of 7 workers running 40 completed episodes per worker and 100 block creation events per episode. For all experiments, we train to completion, then take the average relative reward attained over the last 10 training iterations for each parameter setting (i.e., averaged over 280,000 block creation events).

A. OSM vs. RL

As a starting point, we investigate whether the optimal selfish mining strategy for Bitcoin in the single-agent case (i.e., OSM) dominates a strategy trained with SquirRL. We consider a setting with three agents: agent A is honest, B is running

OSM, and C is using SquirRL. We compare this to a setting where both agents B and C are using OSM. Figure 9 shows the resulting relative rewards for a setting where agents B and C each have fraction $\alpha \leq 0.5$ of the hash power, whereas honest agent has $1 - 2\alpha$. We assume that the follower fractions $\gamma_B = \gamma_C = 0$.

We highlight two observations: first, OSM is no longer optimal against a strategic agent; the RL agent reaps a larger reward than the OSM agent. Compare this to the setting where agents B and C are running OSM, illustrated in Figure 23 for various α . The two-agent game is profitable for both agents when $\alpha \geq 0.38$. However, when agent C is allowed to adapt, it can significantly amplify its own reward at the expense of agent B, actually *reducing* the overall damage to the honest party.

To understand this result, Figure 10 illustrates differences in the OSM and RL strategies. These policy comparison plots should be read as follows: for each pair of actions $(a_{\text{OSM}}, a_{\text{RL}})$ for the two miners, the number in the corresponding square represents $\sum_{s \in \mathcal{S}} I(s, a_{\text{OSM}}, a_{\text{RL}})$ where \mathcal{S} denotes the state space and $I(s, a_{\text{OSM}}, a_{\text{RL}})$ is an indicator variable that equals 1 if a_{OSM} and a_{RL} are the most likely actions taken by OSM and RL agents, respectively, from state s . For Figure 10, we restrict the considered state space to states where the forking characteristic is relevant to make the following policy analysis clearer.

Many of the differences in strategy amount to SquirRL identifying possibilities that are not accounted for in the design of OSM. For example, Figure 10 shows that RL tends to match more than OSM does. This happens because even though both agents have follower fractions equal to zero, the probability of a strategic agent’s fork being extended by some agent is actually nonzero in the multi-agent setting. When the OSM and RL agents are in a tie, the honest miners must choose one of the two chains to mine on. The RL agent recognizes this and chooses to match more often, while the OSM agent does not recognize the potential for others to mine on its chain. Similarly, when the RL agent is in a tie with just the honest party (or both the honest and OSM agents), the other parties can mine on any visible chain. RL recognizes this possibility, but OSM does not. Hence, RL benefits by recognizing and adapting to the new environment.

B. Dual-Agent Adaptive Mining

The previous results suggest that to be competitive, both agents must adapt. Figure 11 illustrates the relative rewards gained when agents B and C are both trained with SquirRL and start with hash power $\alpha \leq 0.5$. Honest player A holds the remaining $1 - 2\alpha$.

Since the strategic agents are symmetric, B and C obtain the same relative rewards on average over many trials. Hence, in this plot, we average the relative rewards of the agent with the *larger* aggregate reward, compared to the average rewards of the agent with *smaller* aggregate reward, and also plot the combined reward of the two. We adopt a similar convention for experiments with more agents. From a protocol security perspective, the combined reward is most important: we want to

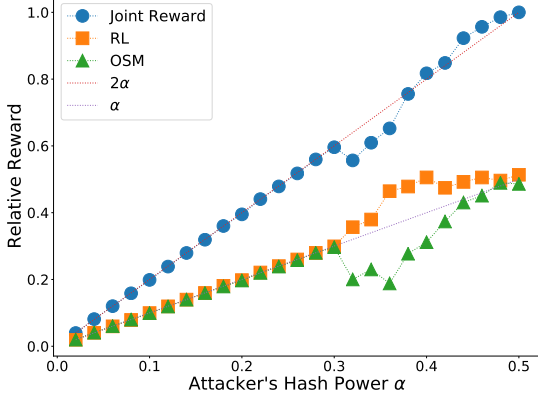


Fig. 9: Relative rewards of OSM vs RL, each starting with α hash power.

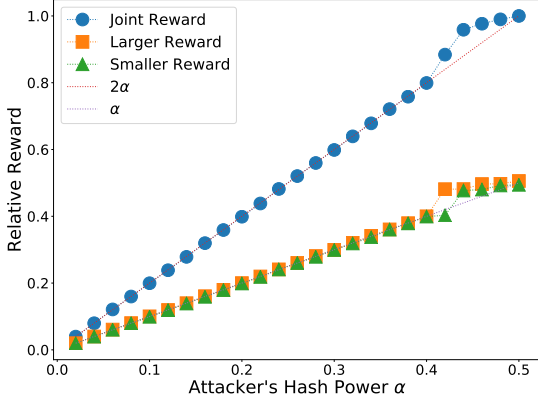


Fig. 11: Relative rewards of RL vs. RL, each starting with α hash power.

design protocols such that selfish agents are not rewarded more than honest agents. Single agent rewards are not as meaningful when the agents are symmetric.

Figure 11 shows that at $\alpha \leq 0.4$, neither agent can outperform honest mining. At $\alpha > 0.4$, the joint reward outperforms honest mining, and when $\alpha \geq 0.42$ both agents individually outperform honest mining. These observations align with how we expect selfish mining profitability to evolve with increasing α : for instance, OSM is profitable in the single agent setting with $\gamma = 0$ when $\alpha > \frac{1}{3}$. Our experiments show that similar results are also true in the multi-agent setting.

In the multi-agent setting with multiple adaptive strategies, individual agents' strategies may not be stable across training iterations, as agents are incentivized to find new strategies to increase their individual rewards in response to new strategies by opposing agents. As such, it is interesting first to understand what strategies emerge in training two competing adaptive agents. Figure 12 illustrates the performance of two such agents with $\alpha = 0.5$ hash power during training. Perhaps surprisingly, we do not observe convergence to a single equilibrium strategy.

	Adopt	Override	Wait	Match
Adopt	7	0	4	0
Override	0	2	1	1
Wait	4	7	6	4
Match	0	0	0	0
	RL			

Fig. 10: Comparison of OSM vs. RL strategies. Each cell corresponds to a given action pair $(a_{\text{OSM}}, a_{\text{RL}})$, and contains the number of states in the state space where this pair is most likely to be executed by the OSM and RL agents respectively.

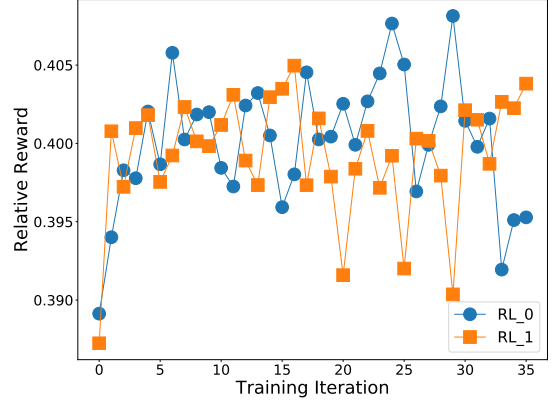


Fig. 12: Relative rewards of RL vs RL, each with $\alpha = 0.4$ hash power as training progresses.

Figure 12 instead illustrates the oscillatory nature of the agents' strategies over time. This suggests (but does not prove) that a pure strategy Nash equilibrium may not exist in the two-strategic-agent setting.

Moreover, we do not observe the agents oscillating between the same two strategies. Figures 21 and 22 in Appendix C show a comparison of the two policies at two different training iterations: 24 and 35. In iteration 24, RL_0 outperforms RL_1 by the largest margin, while the opposite occurs in iteration 35. One might expect by symmetry that the strategies of the dominant players in these two sample iterations would be identical, but our comparison of their respective policies shows that they differ. This observation suggests a possibility borne out by our observations: the strategy space may have a large number of attractors, i.e., strategies to which agents gravitate, rather than a small number among which they oscillate.

C. Multi-Agent Adaptive Mining

Next, we consider the effects of arbitrary $k \geq 2$ strategic agents. This setting was studied in Marmolejo-Cossío et al. [41], where the authors theoretically analyze k agents, each

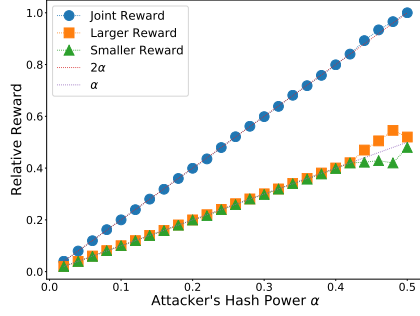


Fig. 13: Relative rewards of RL vs RL with spying, each starting with α hash power and the honest party having the rest. The combined relative reward has dampened from the non-spy case.

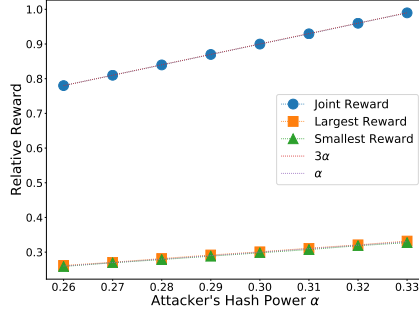


Fig. 14: Relative rewards of RL vs. RL vs. RL, each starting with α hash power and the honest party having the rest. The amount of excess relative reward given to the selfish parties is negligible.

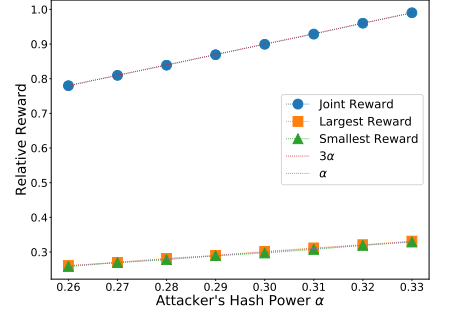


Fig. 15: Relative rewards of RL vs. RL with spying, each starting with α hash power and the honest party having the rest. We see that all agents perform right at the honest level.

of which can use one of two strategies: honest mining or a truncated version of OSM dubbed semi-selfish mining. They find that Nash equilibria exist where all agents perform semi-selfish mining, as long as the agents have enough hash power. For example, when $k = 2$, they find that if both agents have $\alpha > 0.2$ hash power, then it is a Nash equilibrium for all agents to adopt semi-selfish mining. With more agents, the required hash power decreases.

Our experiments with k adaptive miners yield different conclusions. For example, for $k = 2$ agents' combined relative reward to exceed their combined hash power, we find that each agent's hash power should satisfy $\alpha \in (0.4, 0.42)$. Below this threshold, SquirRL consistently returned honest mining policies for all agents. Moreover, for $k > 2$, we found *no* excess combined selfish reward (see e.g. Figure 14, as well as Figures 24-27 in Appendix C).

Despite leading to different conclusions, our findings do not contradict the results of [41]; this is because [41] considers a heavily restricted strategy space, whereas SquirRL has the flexibility to find arbitrary $P(a|s) \forall a, s$. To show the effects of this difference, we ran an experiment similar to the setting of [41], where SquirRL is restricted to two strategies: OSM and honest mining. The resulting strategies are shown in Table III. We see clearly that the Nash equilibrium of this game is for both agents to employ OSM.

Agent 2	Agent 1	
	Honest	OSM
Honest	(0.4, 0.4)	(<0.4, >0.4)
OSM	(>0.4, <0.4)	(0.43, 0.43)

TABLE III: Relative rewards for two parties when they are restricted to OSM and honest mining, both with $\alpha = 0.4, \gamma = 0$. (a, b) represents agent 0 getting reward a and agent 1 getting reward b .

Now return to our setting, where the agents are freely able to choose their strategy. Let agent 0 denote the agent employing OSM, and agent 1 denote the agent employing RL. In Figure

9 we can see that at $\alpha = 0.4$, the RL agent gets a reward of 0.51, while the OSM agent gets a reward of 0.31, and the combined reward is 0.82 (which is less than 0.86, the combined reward if both agents use OSM). RL is able to find a policy that severely damages OSM while enriching itself. Because this strategy exists, both agents playing OSM is **not a Nash equilibrium**. This suggests that it is not sufficient to analyze restrictive strategy spaces such as those considered in [41].

Diminishing rewards for multiple agents. Next, we attempt to explain why honest behavior increasingly emerges as the number of agents grows. Empirically, we observe that the strategies in the multi-agent setting are not exactly honest mining, but they resemble honest mining when the state is close to being "balanced," i.e., when the public chain is at most one block longer or shorter than the strategic agent's chain. For example, Figure 16 shows a representative sample of a strategic agent's policy at the last training iteration for $k = 3$ when the forking state is "relevant". Although the strategy table does not describe honest mining, the upper left corner of the table appears consistent with honest mining. We call this type of strategy *locally honest*. If all parties follow local honesty, then regardless of their remaining policy, the resulting outcome will be indistinguishable from honest mining.

Define a protocol as (k, α, γ) -secure if with k strategic agents, each of hash power $\frac{\alpha}{k}$ and follower fraction $\frac{\gamma}{k}$, the only Nash equilibrium is honest mining. We consider agents with equal resources to avoid the degenerate cases where one agent has an overwhelming majority of the selfish resources, reducing to the one-agent setting. From a protocol developer's perspective, it may be sufficient to design a protocol that is $(k, 1, 0)$ -secure for some k ; this indicates the minimum degree of decentralization needed for incentive mechanism robustness. Our experiments suggest that the Bitcoin protocol may be $(k, 1, 0)$ -secure for $k > 2$ and $(2, 0.8, 0)$ -secure, in addition to the known result of being $(1, \frac{1}{3}, 0)$ -secure [50] (note that as α increases, γ becomes irrelevant). Showing this theoretically is an interesting question for future work.

		Longest Public Chain Length					
		0	1	2	3	4	5
Attacker Private Chain Length	0	Adopt	Adopt	Adopt	Adopt	Adopt	Adopt
	1	Override	Wait	Adopt	Wait	Adopt	Adopt
	2	Override	Override	Adopt	Adopt	Adopt	Adopt
	3	Override	Override	Override	Adopt	Adopt	Adopt
	4	Override	Override	Override	Override	Match	Adopt
	6	Override	Override	Override	Override	Match	Match

Fig. 16: The policy of an agent in the RL vs. RL vs. RL game at the last training iteration.

D. Spy Mining

Thus far, we have assumed that the competing parties have no knowledge of other parties' private chains; this is not always a good assumption. In Bitcoin and other large blockchain networks, *mining pools* have become commonplace, where participants pool their mining resources and divide rewards proportionally. Mining pools are typically open to new participants, and they compete with one another for block rewards. As such, a phenomenon called *spy mining* has emerged, whereby smaller miners participate in a competing mining pool purely to observe its private information, without actually contributing to its mining output.

In our experiments, we model such partial knowledge for the Bitcoin protocol as follows: let s_i be the state observed by agent i without spy knowledge. Then we define the spy mining state s'_i as follows: $s'_i = (s_i || p)$ where p is a tuple of the lengths of the private chains of all the agents, and $||$ refers to the concatenation operation.

In Figure 13, we plot the same graph as Figure 11, except the strategic agents now have access to spy mining information. We observe that the agents' combined rewards over their combined hash power is lower than in the non-spy-mining case. This may be because giving spy information to the miners does not increase their ability to steal relative rewards from the honest parties (whose state is always public by definition), but increases their ability to steal relative reward from other strategic parties. Indeed, we see evidence of this in Figure 13 when $\alpha \geq 0.44$, as the agent with the smaller reward actually receives less relative reward than its own hash power. Compare this to Figure 11, where both agents are able to perform above their hash power when $\alpha > 0.4$.

As before, this effect becomes more pronounced the more agents we add to the system. In experiments for three miners with complete spy information, shown in Figure 15, we see that the combined reward of the selfish miners does not exceed their hash power. Similar results hold for higher numbers of agents; we also plot the spy case for four players in Appendix C, Figure 25.

E. Block Withholding Attacks

Although our focus in this work is on selfish mining attacks, we also applied SquirRL to other classes of incentive-based attacks. In this section, we explore a multi-agent scenario in which agents perform block withholding attacks [13], [24], [33], [38], [49], an attack observed in practice (see, e.g., [60]). In block withholding attacks, a mining pool infiltrates miners into opponent pools to diminish their revenue and gain a competitive advantage. The attacking pool deploys mining resources in a target pool and submits partial solutions, i.e., proofs of work, to earn rewards. If the attacking pool mines a block in the target pool, it withholds it. The target pool thus loses block rewards and revenue relative to its hash power declines.

In prior work, Eyal [13] showed that for two competing mining pools, there is a (unique) Nash equilibrium where each pool assigns a fraction of its resources to infiltrate and sabotage the other. We show that SquirRL automatically learns pool strategies that converge to the same revenues as predicted by that equilibrium.

We adopt the same model as in Eyal [13]. In the two-party version of this model, strategic mining pools P_1 and P_2 each possess "loyal" miners with hash rates of m_1 and m_2 , respectively, $0 \leq m_1 + m_2 \leq 1$. The remaining miners mine on their own, not forming or joining a pool. A miner loyal to pool P_i may either mine honestly in P_i or infiltrate P_{3-i} , as dictated by P_i . When an infiltrating miner loyal to P_i generates a partial block reward, the reward is relayed to P_i and split among all registered miners in P_i , as well as the miners who are loyal to P_i but currently infiltrating P_{3-i} . The goal is to maximize the relative revenue of each miner, normalized by the revenue when there is no block withholding attack.

Denote the hash power of miners loyal to P_i and infiltrating P_{3-i} by x_i . Thus $0 \leq x_i \leq m_i$. We set up the two-agent RL experiment using the reward functions defined in [13]. The normalized relative revenue each miner receives from the mining pool is:

$$r_1(x_1, x_2) = \frac{m_1 m_2 + m_1 x_1 - x_1^2 - x_1 x_2}{(1 - x_1 - x_2)(m_1 m_2 + m_1 x_1 + m_2 x_2)}$$

$$r_2(x_2, x_1) = \frac{m_1 m_2 + m_2 x_2 - x_2^2 - x_1 x_2}{(1 - x_1 - x_2)(m_1 m_2 + m_1 x_1 + m_2 x_2)}.$$

Each agent is assigned a mining hash power m_i and aims to maximize its reward by adapting x_i , the hash power infiltrated into the other pool, from a continuous action space $[0, m_i]$. The reward to be optimized is the immediate result from the normalized relative revenue defined above. There is no state transition in this environment, therefore the episode length of this game is 1. Two agents take turns to adapt their strategies given the best strategy the other agent learned in the last episode. We trained the model using PPO because it is suitable for the multi-agent setting, as mentioned before, and supports continuous action spaces. After 10^6 episodes with learning rate 10^{-6} , both the strategies and rewards converge to those in the Nash equilibrium specified in [13], to within 0.01. The detailed revenues are listed in table IV.

TABLE IV: Normalized mining revenue in a block withholding attack. For two pools with hash rates m_1 and $m_2 = 0.9 - m_1$, the strategies learned by RL lead to a revenue distribution that is close to that predicted by the Nash equilibrium in [13].

		Hash Rate (m_1)			
Reward		0.1	0.2	0.3	0.4
Pool 1	NE	0.48	0.63	0.77	0.89
	RL	0.48	0.63	0.77	0.89
Pool 2	NE	1.04	1.06	1.04	0.99
	RL	1.04	1.06	1.04	0.99

Closely related work in [24] uses RL, specifically a policy gradient based learning method [6], to study block withholding among multiple agents in a setting with dynamic hash rates. A limitation of that work is that it uses a discrete action space, not a continuous one. One interesting feature, on the other hand, is its inclusion of a probabilistic model of migration of unaffiliated (free agent) miners to the most successful pools, an extension of the model in [33]. Unfortunately, this model is rather artificial, with no grounding in empirical study, so we chose not to duplicate it.

VII. RELATED WORK

A number of recent works have analyzed direct attacks on and economic flaws in cryptocurrency protocols.

a) Selfish Mining: The concept of selfish mining was introduced by Eyal and Sirer in [15], and a large body of resulting work has sought to refine related mining models and compute protocol security thresholds in a selfish mining context [44], [45], [48], [50]. Much of this work (including [50]) uses MDP solving to compute optimal selfish mining strategies. These exact solutions are less robust to unexpected, real-time changes in honest hashpower than our RL-based approach. An enhanced model in which two selfish agents and one honest agent exist is considered in [4], but this work does not consider the presence of multiple rational actors in the network, which is far more realistic for a cryptocurrency mining setting. Our techniques allow for reasoning about richer, more realistic models, at the expense of theoretical guarantees. Some work has also proposed mitigations to selfish mining. For example, a new block reward scheme is proposed in [47], but the modifications require heavyweight mining protocol modifications that have proved prohibitive to deployment in practice. Simpler protocol mitigations such as random tie-breaking suggested in [15], on the other hand, have been widely deployed but remain imperfect.

b) General Mining Attacks: A wide range of work has also focused on potential mining attacks besides selfish mining. Many of these attacks can either subsidize a selfish mining attacker’s profit, or compound economic protocol weaknesses exploited by selfish miners, and may lower the required expenditure of attackers. One example is difficulty attacks [22], [43], in which miners can profitably manipulate a chain’s difficulty by secretly raising difficulty on their own private chain [3], switching between competing currencies secured by

the same mining hardware [43], or pausing mining activities around difficulty adjustment time [22]. In some situations, this can lead miners to be completely discouraged from mining on the chain [29]. The study of inducing discouragement in our framework is left to future work.

Another attack involved miner manipulation of user transactions, whether through censorship or reordering, is surveyed in [28]. Many such attacks have been shown in theory, allowing miners to either double-spend user funds or to profit off incorrect assumptions in second-layer applications [5], [36], [42]. Such attacks have been observed in practice [11], [12] and can be performed without hashpower by bribing existing miners [42], [61]. Because these attacks yield direct revenue for miners, they can almost certainly be used to subsidize the profit of a successful mining attack as described in our work, lowering the required hashpower threshold.

Lastly, attacks against miners are possible at the network layer. One example is DoS attacks on mining pools, which have been observed in practice [63] and which more often affect larger pools [27]. Another is eclipse attacks [10], [55], [56], which can ensure a node is connected to only attackers and is applied to blockchain systems in [25], [39]. It has shown that such attacks can interact with selfish mining to increase efficacy [44], and routing-based eclipse attacks have been observed in blockchains [58].

c) RL, MDPs, and Computer Security: The techniques proposed in our paper focus on analyzing multi-agent games using reinforcement learning to refine their security properties. A connection between Markov Decision Processes and RL was made in a seminal paper by Littman [37], which proposes the use of RL to extend MDP analysis to multi-agent games. A body of recent work has applied this technique to cybersecurity actors (eg [52]), attempting to analyze meta-games between attackers and defenders. Our work extends this style of analysis into a setting where multiple “attackers” compete to maximize their own profit share. Unlike in traditional security, our setting is not mutually exclusive (multiple attackers can profit), and requires attackers to continually respond to each others’ actions. This greatly increases the strategy space complexity that must be analyzed, and is likely inherent to the intentional open participation allowed by most cryptocurrency protocols.

VIII. DISCUSSION

Deep reinforcement learning is a promising technique for testing incentive mechanisms in blockchain protocols. In this work, we propose SquirRL, a deep RL-based framework for the automated detection of vulnerabilities in blockchain incentive mechanisms. We have shown that SquirRL can approximate known theoretical results about attacks on blockchain incentive mechanisms, while also extending to settings that are not tractable using classical techniques like MDP solvers. For example, it gives new results and insights in settings with multiple competing agents, a problem that has remained theoretically intractable due to its large state space and the repeated nature of the game.

However, our approach exhibits a key weakness: experimental results showing that a protocol is secure cannot be taken as proof that it is secure. This is related to the observation that deep reinforcement learning algorithms are known to be sensitive to hyperparameters. While recent algorithms like PPO [51] have been designed with hyperparameter robustness in mind, this is still a big area of research. From a protocol testing perspective, the fact that the RL agents do not find an exploit could be the result of a secure protocol or bad hyperparameters. Hence, we view SquirRL primarily as a “quick and dirty” tool allowing protocol designers to gain some intuition about their protocol in cases where theoretical analysis is infeasible.

In addition to this caveat, several important questions remain. Principal among them is understanding the effects of cooperation among agents. Our multi-agent experiments have thus far been limited to competing agents; we assume that if two agents collude, they collude completely, which is equivalent to having fewer competing agents. However, in reality, there are cases where agents may partially cooperate, e.g., by sharing incomplete information. This setting is straightforward to model using SquirRL, and is a natural direction for future work. Other important directions include modeling agents who attempt to maximize their per-unit-time reward, as well as agents who launch other classes of incentive-based attacks, such as time-bandit attacks [11].

ACKNOWLEDGMENTS

The authors would like to thank the Army Research Office under grant W911NF-18-1-0332-(73198-NS), the National Science Foundation under grants CCF-1705007, CNS-1564102, CNS-1704615, CNS-1933655 and the Initiative for Cryptocurrencies and Contracts (IC3) for their support.

REFERENCES

- [1] Ethereum 2.0 phase 0 – the beacon chain. <https://github.com/ethereum/eth2.0-specs/issues/433>.
- [2] Ethereum 2.0 implementers call 12 notes, 2019. https://github.com/ethereum/eth2.0-pm/blob/master/eth2.0-implementers-calls/call_012.md.
- [3] Lear Bahack. Theoretical bitcoin attacks with less than half of the computational power (draft). *arXiv preprint arXiv:1312.7013*, 2013.
- [4] Qianlan Bai, Xinyan Zhou, Xing Wang, Yuedong Xu, Xin Wang, and Qingsheng Kong. A deep dive into blockchain selfish mining. *arXiv preprint arXiv:1811.08263*, 2018.
- [5] Joseph Bonneau. Why buy when you can rent? In *International Conference on Financial Cryptography and Data Security*, pages 19–26. Springer, 2016.
- [6] Michael Bowling and Manuela Veloso. Scalable learning in stochastic games. In *AAAI Workshop on Game Theoretic and Decision Theoretic Agents*, pages 11–18, 2002.
- [7] Greg Brockman, Vicki Cheung, Ludwig Pettersson, Jonas Schneider, John Schulman, Jie Tang, and Wojciech Zaremba. Openai gym, 2016.
- [8] Vitalik Buterin and Virgil Griffith. Casper the friendly finality gadget. *arXiv preprint arXiv:1710.09437*, 2017.
- [9] Miles Carlsten, Harry Kalodner, S Matthew Weinberg, and Arvind Narayanan. On the instability of bitcoin without the block reward. In *Proceedings of the 2016 ACM SIGSAC Conference on Computer and Communications Security*, pages 154–167. ACM, 2016.
- [10] Miguel Castro, Peter Druschel, Ayalvadi Ganesh, Antony Rowstron, and Dan S Wallach. Secure routing for structured peer-to-peer overlay networks. *ACM SIGOPS Operating Systems Review*, 36(SI):299–314, 2002.
- [11] Philip Daian, Steven Goldfeder, Tyler Kell, Yunqi Li, Xueyuan Zhao, Iddo Bentov, Lorenz Breidenbach, and Ari Juels. Flash boys 2.0: Frontrunning, transaction reordering, and consensus instability in decentralized exchanges. *arXiv preprint arXiv:1904.05234*, 2019.
- [12] Shayan Eskandari, Seyedehmahsa Moosavi, and Jeremy Clark. Sok: Transparent dishonesty: front-running attacks on blockchain. 2019.
- [13] Ittay Eyal. The miner’s dilemma. In *2015 IEEE Symposium on Security and Privacy*, pages 89–103. IEEE, 2015.
- [14] Ittay Eyal and Emin Gün Sirer. How to detect selfish miners, 2014. <http://hackingdistributed.com/2014/01/15/detecting-selfish-mining/>.
- [15] Ittay Eyal and Emin Gün Sirer. Majority is not enough: Bitcoin mining is vulnerable. *Communications of the ACM*, 61(7):95–102, 2018.
- [16] Vincent François-Lavet, Peter Henderson, Riashat Islam, Marc G Belle-mare, Joelle Pineau, et al. An introduction to deep reinforcement learning. *Foundations and Trends® in Machine Learning*, 11(3-4):219–354, 2018.
- [17] Juan Garay, Aggelos Kiayias, and Nikos Leonardos. The bitcoin backbone protocol: Analysis and applications. In *Annual International Conference on the Theory and Applications of Cryptographic Techniques*, pages 281–310. Springer, 2015.
- [18] Arthur Gervais, Ghassan O Karame, Karl Wüst, Vasileios Glykantzis, Hubert Ritzdorf, and Srdjan Capkun. On the security and performance of proof of work blockchains. In *Proceedings of the 2016 ACM SIGSAC conference on computer and communications security*, pages 3–16. ACM, 2016.
- [19] Yossi Gilad, Rotem Hemo, Silvio Micali, Georgios Vlachos, and Nickolai Zeldovich. Algorand: Scaling byzantine agreements for cryptocurrencies. In *Proceedings of the 26th Symposium on Operating Systems Principles*, pages 51–68. ACM, 2017.
- [20] Yossi Gilad, Rotem Hemo, Silvio Micali, Georgios Vlachos, and Nickolai Zeldovich. Algorand: Scaling byzantine agreements for cryptocurrencies. In *Proceedings of the 26th Symposium on Operating Systems Principles*, pages 51–68. ACM, 2017.
- [21] Guy Goren and Alexander Spiegelman. Mind the mining. In *Proceedings of the 2019 ACM Conference on Economics and Computation*, EC ’19, pages 475–487. New York, NY, USA, 2019. ACM.
- [22] Guy Goren and Alexander Spiegelman. Mind the mining. *arXiv preprint arXiv:1902.03899*, 2019.
- [23] Cyril Grunspan and Ricardo Pérez-Marco. Selfish mining in ethereum. *arXiv preprint arXiv:1904.13330*, 2019.
- [24] Alireza Toroghi Haghighat and Mehdi Shajari. Block withholding game among bitcoin mining pools. *Future Generation Computer Systems*, 97:482–491, 2019.
- [25] Ethan Heilman, Alison Kendler, Aviv Zohar, and Sharon Goldberg. Eclipse attacks on bitcoin’s peer-to-peer network. In *24th {USENIX} Security Symposium ({USENIX} Security 15)*, pages 129–144, 2015.
- [26] Van L Jacobson and Diana K Smetters. Controlling the spread of interests and content in a content centric network, September 27 2016. US Patent 9,456,054.
- [27] Benjamin Johnson, Aron Laszka, Jens Grossklags, Marie Vasek, and Tyler Moore. Game-theoretic analysis of ddos attacks against bitcoin mining pools. In *International Conference on Financial Cryptography and Data Security*, pages 72–86. Springer, 2014.
- [28] Aljosha Judmayer, Nicholas Stifter, Alexei Zamyatin, Itay Tsabary, Ittay Eyal, Peter Gaži, Sarah Meiklejohn, and Edgar Weippl. Pay-to-win: Incentive attacks on proof-of-work cryptocurrencies. 2019.
- [29] Igor Kabashkin. Risk modelling of blockchain ecosystem. In *International Conference on Network and System Security*, pages 59–70. Springer, 2017.
- [30] Ido Kaiser. A decentralized private marketplace. 2017.
- [31] Tamás Király and Lilla Lomoschitz. Profitability of the coin-hopping strategy. *EGRES quick proof*, (2018-03), 2018.
- [32] Vijay R Konda and John N Tsitsiklis. Actor-critic algorithms. In *Advances in neural information processing systems*, pages 1008–1014, 2000.
- [33] Aron Laszka, Benjamin Johnson, and Jens Grossklags. When bitcoin mining pools run dry. In *International Conference on Financial Cryptography and Data Security*, pages 63–77. Springer, 2015.
- [34] Chenxing Li, Peilun Li, Dong Zhou, Wei Xu, Fan Long, and Andrew Yao. Scaling nakamoto consensus to thousands of transactions per second. *arXiv preprint arXiv:1805.03870*, 2018.
- [35] Eric Liang, Richard Liaw, Philipp Moritz, Robert Nishihara, Roy Fox, Ken Goldberg, Joseph E. Gonzalez, Michael I. Jordan, and Ion Stoica. RLlib: Abstractions for Distributed Reinforcement Learning. *arXiv e-prints*, page arXiv:1712.09381, Dec 2017.

- [36] Kevin Liao and Jonathan Katz. Incentivizing blockchain forks via whale transactions. In *International Conference on Financial Cryptography and Data Security*, pages 264–279. Springer, 2017.
- [37] Michael L Littman. Markov games as a framework for multi-agent reinforcement learning. In *Machine learning proceedings 1994*, pages 157–163. Elsevier, 1994.
- [38] Loi Luu, Ratul Saha, Inian Parameshwaran, Prateek Saxena, and Aquinas Hobor. On power splitting games in distributed computation: The case of bitcoin pooled mining. In *2015 IEEE 28th Computer Security Foundations Symposium*, pages 397–411. IEEE, 2015.
- [39] Yuval Marcus, Ethan Heilman, and Sharon Goldberg. Low-resource eclipse attacks on ethereum’s peer-to-peer network. *IACR Cryptology ePrint Archive*, 2018:236, 2018.
- [40] Marlow. Why selfish miners do not exist and never will. <https://medium.com/@ProfFaustus/why-selfish-miners-do-not-exist-and-never-will-6d68b5ad571c>, 2018.
- [41] Francisco J. Marmolejo-Cossio, Eric Brigham, Benjamin Sela, and Jonathan Katz. Competing (Semi)-Selfish Miners in Bitcoin. *arXiv e-prints*, page arXiv:1906.04502, Jun 2019.
- [42] Patrick McCorry, Alexander Hicks, and Sarah Meiklejohn. Smart contracts for bribing miners. In *International Conference on Financial Cryptography and Data Security*, pages 3–18. Springer, 2018.
- [43] Dmitry Meshkov, Alexander Chepur, and Marc Jansen. Short paper: Revisiting difficulty control for blockchain systems. In *Data Privacy Management, Cryptocurrencies and Blockchain Technology*, pages 429–436. Springer, 2017.
- [44] Kartik Nayak, Srikanth Kumar, Andrew Miller, and Elaine Shi. Stubborn mining: Generalizing selfish mining and combining with an eclipse attack. In *2016 IEEE European Symposium on Security and Privacy (EuroS&P)*, pages 305–320. IEEE, 2016.
- [45] Jianyu Niu and Chen Feng. Selfish mining in ethereum. *arXiv preprint arXiv:1901.04620*, 2019.
- [46] Rafael Pass and Elaine Shi. Fruitchains: A fair blockchain. In *Proceedings of the ACM Symposium on Principles of Distributed Computing*, pages 315–324. ACM, 2017.
- [47] Rafael Pass and Elaine Shi. Fruitchains: A fair blockchain. In *Proceedings of the ACM Symposium on Principles of Distributed Computing*, pages 315–324. ACM, 2017.
- [48] Fabian Ritz and Alf Zugenmaier. The impact of uncle rewards on selfish mining in ethereum. In *2018 IEEE European Symposium on Security and Privacy Workshops (EuroS&PW)*, pages 50–57. IEEE, 2018.
- [49] Meni Rosenfeld. Analysis of bitcoin pooled mining reward systems. *arXiv preprint arXiv:1112.4980*, 2011.
- [50] Ayelet Sapirshstein, Yonatan Sompolsky, and Aviv Zohar. Optimal selfish mining strategies in bitcoin. In *International Conference on Financial Cryptography and Data Security*, pages 515–532. Springer, 2016.
- [51] John Schulman, Filip Wolski, Prafulla Dhariwal, Alec Radford, and Oleg Klimov. Proximal Policy Optimization Algorithms. *arXiv e-prints*, page arXiv:1707.06347, Jul 2017.
- [52] Sajjan Shiva, Sankar Das Roy, and Dipankar Dasgupta. Game theory for cyber security. In *Proceedings of the Sixth Annual Workshop on Cyber Security and Information Intelligence Research*, page 34. ACM, 2010.
- [53] David Silver, Aja Huang, Chris J Maddison, Arthur Guez, Laurent Sifre, George Van Den Driessche, Julian Schrittwieser, Ioannis Antonoglou, Veda Panneershelvam, Marc Lanctot, et al. Mastering the game of go with deep neural networks and tree search. *nature*, 529(7587):484, 2016.
- [54] David Silver, Thomas Hubert, Julian Schrittwieser, Ioannis Antonoglou, Matthew Lai, Arthur Guez, Marc Lanctot, Laurent Sifre, Dhruv Kumar, Thore Graepel, et al. Mastering chess and shogi by self-play with a general reinforcement learning algorithm. *arXiv preprint arXiv:1712.01815*, 2017.
- [55] Atul Singh et al. Eclipse attacks on overlay networks: Threats and defenses. In *IEEE INFOCOM*. Citeseer, 2006.
- [56] Emil Sit and Robert Morris. Security considerations for peer-to-peer distributed hash tables. In *International Workshop on Peer-to-Peer Systems*, pages 261–269. Springer, 2002.
- [57] Yonatan Sompolsky and Aviv Zohar. Secure high-rate transaction processing in bitcoin. In *International Conference on Financial Cryptography and Data Security*, pages 507–527. Springer, 2015.
- [58] JOE STEWART. BGP hijacking for cryptocurrency profit. <https://www.secureworks.com/research/bgp-hijacking-for-cryptocurrency-profit>, Aug 2014.
- [59] Richard S Sutton, David A McAllester, Satinder P Singh, and Yishay Mansour. Policy gradient methods for reinforcement learning with function approximation. In *Advances in neural information processing systems*, pages 1057–1063, 2000.
- [60] Lillian Teng. F2Pool founder condemns block withholding attacks performed by some chinese mining pools on its competitors. <https://news.8btc.com/f2pool-founder-condemns-block-withholding-attacks-performed-by-some-chinese-mining-pools-on-its-competitors>, June 2019.
- [61] Jason Teutsch, Sanjay Jain, and Prateek Saxena. When cryptocurrencies mine their own business. In *International Conference on Financial Cryptography and Data Security*, pages 499–514. Springer, 2016.
- [62] Hado van Hasselt, Arthur Guez, and David Silver. Deep Reinforcement Learning with Double Q-learning. *arXiv e-prints*, page arXiv:1509.06461, Sep 2015.
- [63] Marie Vasek, Micah Thornton, and Tyler Moore. Empirical analysis of denial-of-service attacks in the bitcoin ecosystem. In *International conference on financial cryptography and data security*, pages 57–71. Springer, 2014.
- [64] Pavel Vasin. Blackcoin’s proof-of-stake protocol v2. URL: <https://blackcoin.co/blackcoin-pos-protocol-v2-whitepaper.pdf>, 71, 2014.
- [65] Christopher JCH Watkins and Peter Dayan. Q-learning. *Machine learning*, 8(3-4):279–292, 1992.
- [66] CC White. *Markov decision processes*. Springer, 2001.
- [67] Ronald J Williams. Simple statistical gradient-following algorithms for connectionist reinforcement learning. *Machine learning*, 8(3-4):229–256, 1992.
- [68] Gavin Wood. Polkadot: Vision for a heterogeneous multi-chain framework.
- [69] Gavin Wood. Chain reorganisation depth expectations, 2015. <https://blog.ethereum.org/2015/08/08/chain-reorganisation-depth-expectations/>.
- [70] Gavin Wood et al. Ethereum: A secure decentralised generalised transaction ledger.
- [71] Gavin Wood et al. Ethereum: A secure decentralised generalised transaction ledger. *Ethereum project yellow paper*, 151(2014):1–32, 2014.
- [72] Yuhuai Wu, Elman Mansimov, Roger B Grosse, Shun Liao, and Jimmy Ba. Scalable trust-region method for deep reinforcement learning using kronecker-factored approximation. In *Advances in neural information processing systems*, pages 5279–5288, 2017.

APPENDIX

A. Proof of Proposition IV.1

As mentioned before, we use the deterministic analysis of [21]. This analysis deals entirely with expectations, and abstracts away the randomness in block time generation; it is a good approximation when the epoch duration is high (as it is in Bitcoin). We denote the number of main chain blocks generated by the attacker during the i th epoch as $B_a(i)$ (assuming $1 \leq i \leq n$) and the number of stale blocks generated by the attacker as $S_a(i)$; we suppress the notation p for simplicity. Here a stale block refers to any block that does not end up on the main chain. Those numbers for the honest miner are $B_h(n)$ and $S_h(n)$. We have $B_a(n) + B_h(n) = M, n \in \mathbb{N}_+$ since every epoch has M of blocks in the main chain.

In the first epoch, the average block generation time is T_0 , but the main chain growth rate may be lower than $1/T_0$ if the attacker deviates from the honest mining protocol. Therefore, the total duration of the first epoch is $D_1 = (M + S_a(1) + S_h(1))T_0$. After the first difficulty adjustment, the difficulty will be multiplied by $M/(M + S_a(1) + S_h(1))$, so the expected duration of the second epoch is

$$D_2 = (M + S_a(2) + S_h(2))T_0 \frac{M}{(M + S_a(1) + S_h(1))}.$$

Recall that the attacker uses the same strategy in epochs 1 and 2 and the honest miner is also repeating its strategy, so we have

$B_a(1) = B_a(2), B_h(1) = B_h(2), S_a(1) = S_a(2), S_h(1) = S_h(2)$ under deterministic analysis [21]. We therefore use the simplified notation B_a, B_h, S_a, S_h and suppress notation n . Therefore, the total time for the second epoch is actually MT_0 . This pattern holds for larger n by induction. We can therefore write the absolute reward rate of the attacker for n epochs R_n as follows:

$$\begin{aligned} R_n &= \frac{nB_a}{(M + S_a + S_h)T_0 + (n-1)MT_0} \\ &= \frac{nB_a}{nMT_0 + (S_a + S_h)T_0} \\ &= \frac{1}{T_0} \frac{B_a}{(B_a + B_h) + \frac{1}{n}(S_a + S_h)}. \end{aligned} \quad (2)$$

Notice that optimizing the absolute reward rate for n epochs R_n is equivalent to optimizing $T_0 R_n$, since this just scales the objective by a constant. Computing the difference between \tilde{R}_n and $T_0 R_n$, we get

$$\begin{aligned} |T_0 R_n - \tilde{R}_n| &= \frac{B_a}{B_a + B_h} - \frac{B_a}{(B_a + B_h) + \frac{1}{n}(S_a + S_h)} \\ &= \frac{B_a(B_a + B_h + \frac{1}{n}(S_a + S_h)) - B_a(B_a + B_h)}{(B_a + B_h + \frac{1}{n}(S_a + S_h))(B_a + B_h)} \\ &\leq \frac{M(\frac{M}{n})}{M^2} = \frac{1}{n} \end{aligned} \quad (3)$$

where (3) follows because $B_a + B_h = M$ and $S_a + S_h \leq M$. This gives the claim.

B. Stochastic Hash Power in Real Cryptocurrencies

Here, we provide the visualization results of the total hash power and the relative hash power of the attacker for the Bitcoin, Litecoin, Dogecoin and Vertcoin tests in Sec. V-D.

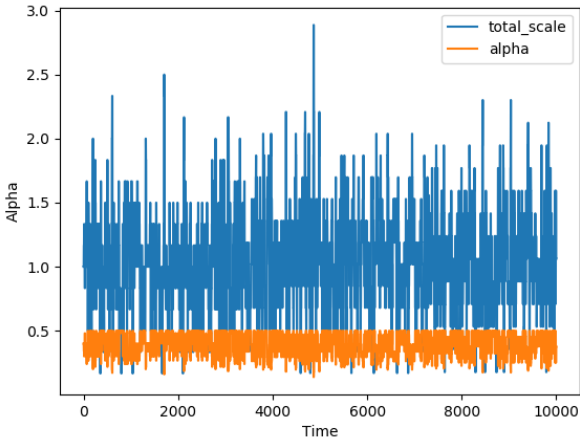


Fig. 17: The total hash rate fluctuation(normalized) and the relative hash power for the attacker with initial $\alpha = 0.4$ in Bitcoin from Sep. 2018 to Oct. 2018.

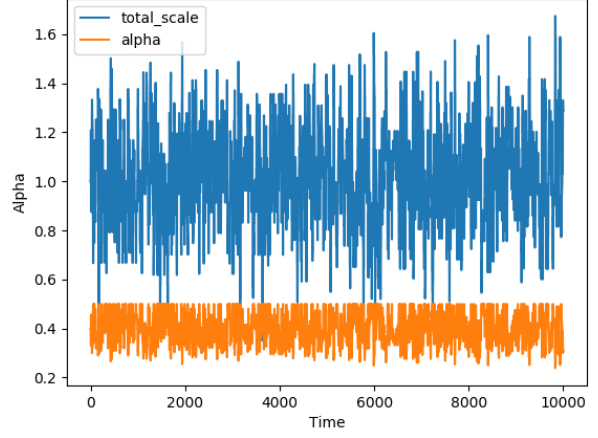


Fig. 18: The total hash rate fluctuation(normalized) and the relative hash power for the attacker with initial $\alpha = 0.4$ in Litecoin from Sep. 2018 to Oct. 2018.

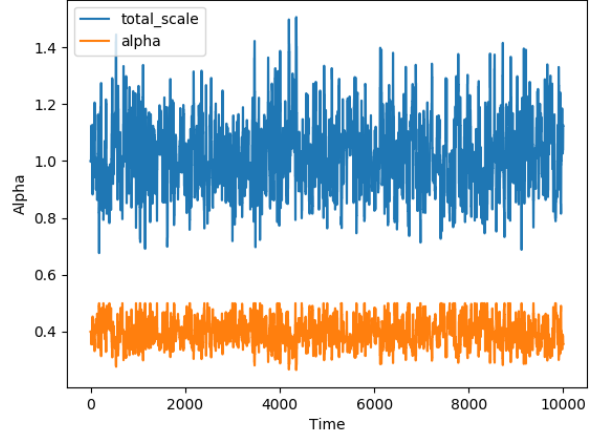


Fig. 19: The total hash rate fluctuation(normalized) and the relative hash power for the attacker with initial $\alpha = 0.4$ in Dogecoin from Sep. 2018 to Oct. 2018.

C. Multi-agent Selfish Mining

In this section we include additional experimental results on the $k \geq 2$ setting. For $k = 4, 6, 8$ we see that the trend that we saw from $k = 3$ continues: the agents are unable to settle upon a equilibrium other than honest mining.

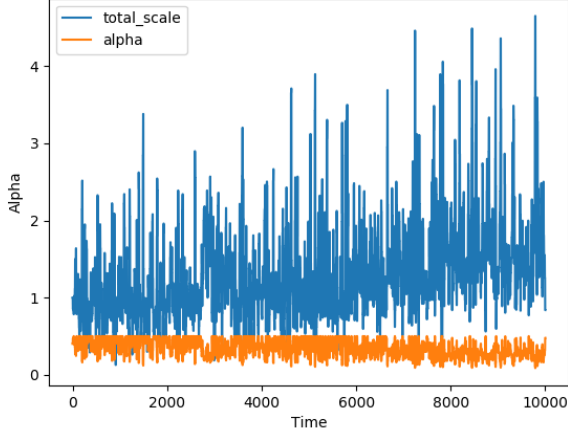


Fig. 20: The total hash rate fluctuation(normalized) and the relative hash power for the attacker with initial $\alpha = 0.4$ in Vertcoin from Sep. 2018 to Oct. 2018.

	Adopt	Override	Wait	Match
Adopt	72	0	26	10
Override	0	111	10	14
Wait	8	10	20	22
Match	0	0	0	0

RL_1

Fig. 21: Comparison of RL vs. RL strategies at training iteration 24. RL_0 is winning more blocks here. Compared to Figure 22, we can see RL_1 is waiting less (is less aggressive).

	Adopt	Override	Wait	Match
Adopt	77	0	28	4
Override	0	105	20	10
Wait	5	5	29	20
Match	0	0	0	0

RL_1

Fig. 22: Comparison of RL vs. RL strategies at training iteration 35. RL_1 is winning more blocks here. Compared to Figure 21, RL_1 is waiting more (is more aggressive).

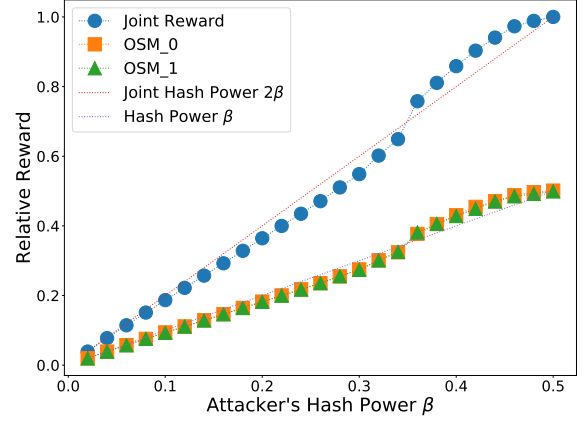


Fig. 23: Relative rewards of OSM vs. OSM, each starting with β hash power and the honest party having the rest. We can see that both parties do worse honest mining at $\beta \leq 0.34$ and outperform honest mining at $\beta \geq 0.36$. Note this does not contradict the single player case, as there is another dishonest agent.

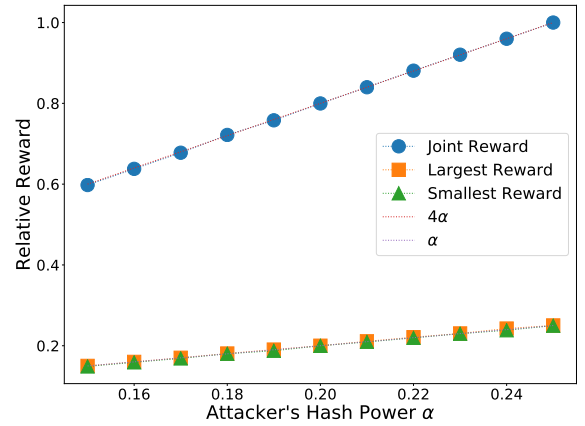


Fig. 24: Relative rewards of four RL agents, each starting with β hash power and the honest party having the rest. We see that all agents perform right at the honest level, and under inspection the policies do reflect an honest equilibrium.

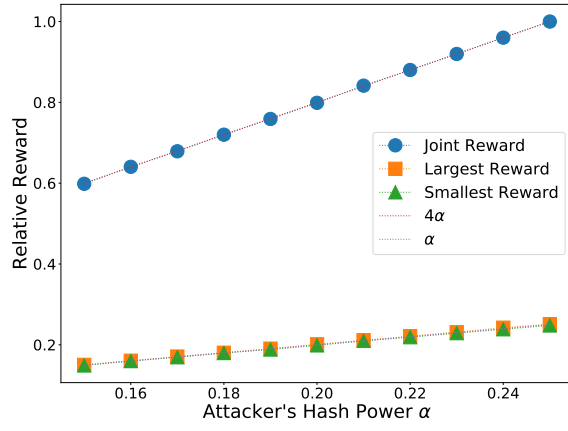


Fig. 25: Relative rewards of four RL agents with spying, each starting with β hash power and the honest party having the rest.

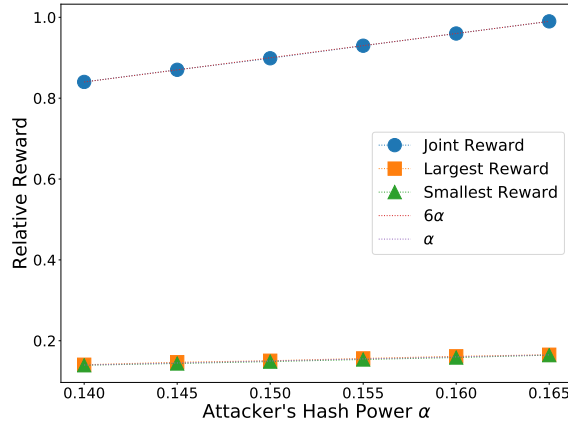


Fig. 26: Relative rewards of six RL agents, each starting with β hash power and the honest party having the rest. We see that all agents perform right at the honest level, and under inspection the policies do reflect an honest equilibrium.

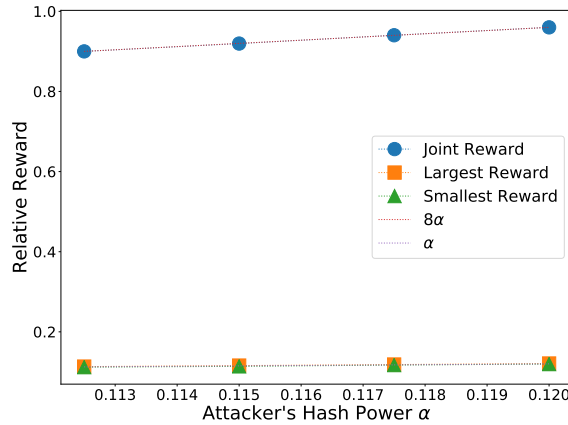


Fig. 27: Relative rewards of eight RL agents, each starting with β hash power and the honest party having the rest. We see that all agents perform right at the honest level, and under inspection the policies do reflect an honest equilibrium.